https://doi.org/10.5194/egusphere-2025-1339
Preprint. Discussion started: 28 March 2025

Comparative Analysis of Continuous and Reinitialized Dynamical Downscaling in the North Atlantic and Surrounding Continents

Brieuc Thomas[1,*], Jose Carlos Fernández-Alvarez[2,1,3], Xurxo Costoya[1], Maite deCastro[1], Raquel Nieto[1], David Carvalho[3], Luis Gimeno[1], Moncho Gómez-Gesteira[1]

[1]Centro de Investigación Mariña, Universidade de Vigo, Environmental Physics Laboratory (EPhysLab), Campus da Auga, 32004, Ourense, Spain
[2]Galicia Supercomputing Center (CESGA), Santiago de Compostela, Spain
[3]CESAM, Departamento de Física, Universidad de Aveiro, 3810-193, Aveiro, Portugal

Correspondence to: Brieuc Thomas (brieuc.thomas@uvigo.es)

Abstract. General Circulation Models provide comprehensive climate projections but are limited by coarse spatial resolution. To address this issue, Regional Climate Models are used for higher-resolution simulations, particularly to assess regional climate change impacts. This process, called dynamical downscaling, typically involves continuous simulations over a selected period. Alternatively, multiple reinitialized simulations over shorter intervals can be employed to minimize error accumulation and reduce computation time through parallel processing. However, this approach may hinder the development of certain atmospheric phenomena. In this study, the Weather Research and Forecasting model was used for continuous and daily reinitialized dynamical downscaling. Simulations were driven by ERA5 and Coupled Model Intercomparison Project Phase 6 data at 1º and 1.25º spatial resolution, respectively, covering 115ºW-40ºE in longitude and 20ºN-60ºN latitude, and downscaled to 20-km resolution. The results were evaluated against ERA5 data at 0.25° resolution to assess accuracy. The analysis focused on wind speed, temperature, humidity, precipitation, surface pressure, and solar radiation. Overall, both techniques demonstrated good to excellent correlation with the reference data. However, neither method reliably captured wind speed nor surface pressure in mountainous areas. In ERA5-driven simulations, the reinitialized technique performed better than the continuous for air temperature and humidity in coastal regions, whereas the continuous approach showed a slight advantage in estimating solar radiation across all surfaces. For CMIP6-driven simulations, both downscaling techniques produced similar results, except for solar radiation and over land, where the continuous method demonstrated marginally better performance. Considering the significantly lower computational cost of the reinitialized method - approximately 30 times less in this study - it is recommended as the preferred approach when its performance is comparable to or better than that of the continuous method.

1 Introduction

The heavy reliance on fossil fuels as the primary energy source greatly accelerates climate change by emitting greenhouse gases (GHGs) into the atmosphere (IPCC, 2021). While the most well-known effect is the global rise in air temperature, all

https://doi.org/10.5194/egusphere-2025-1339
Preprint. Discussion started: 28 March 2025

atmospheric variables are impacted by these altered conditions, therefore influencing many economic and societal sectors (Schewe et al., 2019). Understanding how climate change may influence atmospheric characteristics is therefore crucial. Climate models have proven to be the most effective and reliable tools for tackling this challenge (Zhang & Li, 2021). General Circulation Models (GCMs) are particularly powerful as they provide future climate projections. Among them, the 6th phase of the Coupled Model Intercomparison Project (CMIP6) (Eyring et al., 2016) offers the latest and most comprehensive set of GCMs. These models provide atmospheric climate projections based on diverse Shared Socioeconomic Pathways (SSPs) (Riahi et al., 2017). SSPs evaluate future GHG emissions by considering a range of factors, including population growth, education, urbanization, and economic changes, such as Gross Domestic Product (GDP), under varying policy assumptions. However, simulating the entire Earth's atmosphere comes with a significant computational cost, resulting in GCMs offering relatively coarse spatial resolution, which limits their effectiveness for regional climate studies. To achieve higher-resolution data that accounts for regional specifics, dynamical downscaling is employed. This involves using a Regional Climate Model (RCM) driven by lower-resolution GCM data to simulate the atmosphere at a finer spatial scale for a targeted area (Jacob et al., 2014). Nevertheless, it is crucial to validate the performance of climate models in accurately replicating atmospheric trends in a specific region. This validation involves comparing historical model outputs with regional observational data. Models that closely match observed data are considered reliable for reflecting actual conditions and are thus suitable for predicting future atmospheric trends (Thomas et al., 2023).

Atmospheric modelers typically use several methods for dynamical downscaling. The most common approach involves conducting a continuous simulation. However, this can lead to error accumulation over time: as the simulation progresses, models often deviate from the initial input data used to drive them (Spero et al., 2018). To mitigate this issue, a nudging correction can be applied, which comes in two forms. Analysis nudging (Deng et al., 2007) guides the model toward alignment by minimizing differences between the simulated fields and the interpolated reference data in both space and time at each grid point. On the other hand, spectral nudging (Miguez-Macho et al., 2004) addresses model drift by decomposing mismatches into Fourier components and selectively adjusting the larger-scale, low-frequency features to match the reference data. Both the application of analysis (Bullock et al., 2014; Wooten et al., 2016) and spectral nudging (Glisan et al., 2013; Spero et al., 2014) improve the dynamical downscaling simulations when compared to no nudging at all, while spectral nudging is in theory the most advantageous method in regional climate modeling, because it targets only the large-scale, resolvable features in the driving data (Spero et al., 2018). Another dynamical downscaling approach is to conduct a series of independent, short simulations rather than a single continuous long run. This method has the primary advantage of preventing error accumulation since the individual simulation periods are much shorter. Additionally, it can reduce the overall modeling time, as these shorter simulations can be run in parallel on multiple cores (Jerez et al., 2020). However, this approach has limitations, including the potential inability of the RCM to develop certain long-term physical processes, such as surface hydrological cycles (Christensen, 1999), or convection for instance, due to the frequent resetting of the model's

https://doi.org/10.5194/egusphere-2025-1339
Preprint. Discussion started: 28 March 2025

variable memory. The reinitialized approach was used in several studies to perform dynamical downscaling, showing great accuracy in the modeled data, for instance for winds (Horvath et al., 2012; Thomas et al., 2023; Thomas et al., 2025).

Some studies compared continuous and reinitialized dynamical downscaling techniques. Pan et al. (1999) performed a whole range of simulations for a 1-month period in the US, from one continuous monthly run to thirty daily runs. They analysed several atmospheric variables and demonstrated the feasibility of dividing a long climate simulation into a set of shorter ones, when a long-enough disposable spin-up period is respected. In South America, Qian et al. (2003) ran a 5-month simulation continuously, in five monthly parts, and in several 10-day chunks. They showed that most reinitialized simulations resulted in the most accurate precipitation values. Both these studies applied spectral nudging when performing continuous dynamical downscaling. Lo et al. (2008) modelled an entire year in the US and found that, when no nudging is considered, the reinitialized runs showed better results than the continuous one, except for soil parameters. Additionally, more frequent reinitialization gives better results. When applying analysis nudging, the reinitialized and continuous runs present highly similar values. Analysing two one-month (winter and summer) wind simulations in Portugal, Carvalho et al. (2012) demonstrated that the best numerical configuration consisted in grid nudging applied to reinitialized simulations no longer than two days. As for Lucas-Picher et al. (2013), they modelled precipitation using both daily-reinitialized (with 6h spin-up period) and continuous (without any kind of nudging) dynamical downscaling techniques for a 30-year historical period in Europe. They showed that the use of the reinitialized method improved the temporal correlation with observational data, and showed lower systematic errors than the continuous one. Lastly, Liu et al. (2018) showed that, over China, a daily-reinitialized dynamical downscaling with 12h spin-up period showed the smaller error for air temperature and humidity than a continuous dynamical downscaling with spectral nudging. The opposite occurs for precipitation. To validate their results, all the aforementioned studies relied on observational data, which differs from the data used to drive the RCM. While this approach has merit, it introduces a potential issue: the RCM output might be accurately dynamically downscaled but still differ significantly from the data used for comparison. As a result, these studies do not determine which dynamical downscaling technique performs best but rather which produces outputs most similar to the chosen validation data. To address the first question, the same dataset - at different spatial resolutions - should be used both to drive the RCM (low-resolution data) and to validate its outputs (high-resolution data).

This study aims to assess the performance of two dynamical downscaling processes to reproduce key meteorological variables from both reanalysis and climatological datasets, and to identify which approach provides superior dynamical downscaling performance. These approaches are a continuous method with spectral nudging and a daily-reinitialized method, using the WRF-ARW v4.3.3 model (Skamarock et al., 2021) forced with ERA5 reanalysis dataset at 1º (Hersbach et al., 2020) and a CMIP6 multi-model ensemble at 1.25º (Xu et al., 2021). Specifically, the dynamical downscaling is configured to produce outputs at a 20-km spatial resolution, comparable to the native 0.25º resolution of ERA5, to which the results are compared. The analysis focuses on several variables, including wind speed, air temperature, humidity,

https://doi.org/10.5194/egusphere-2025-1339
Preprint. Discussion started: 28 March 2025

precipitation, atmospheric pressure, and solar radiation. Simulations will cover the year 2014 with a 6-hour temporal resolution, over a domain spanning the North Atlantic and adjacent continental regions (from -115ºW to 40ºE in longitude and 60ºN to 20ºN in latitude).

2. Data and Methods

2.1. WRF model setup

To perform the dynamical downscalings, the WRF-ARW v4.3.3 meteorological model was fed by initial and boundary conditions from the ERA5 reanalysis dataset. Even though it provides data at a 0.25º spatial resolution, only one out of four grid points were used (both in longitude and latitude), so that the input data of the WRF model have a 1º spatial resolution. It also provides data at a 1-hour resolution, but only data at 00:00, 06:00, 12:00 and 18:00 UTC (thus with a 6-hour temporal resolution) were used to initialize WRF. The WRF model was also forced with a CMIP6 multi-model ensemble provided by Xu et al. (2021). It has a spatial resolution of 1.25º and a temporal resolution of 6 hours and encompasses historical records until 2014. To analyse long-term trends, they utilized a multi-model ensemble of 18 GCMs from the CMIP6 project. Additionally, bias correction was applied using ERA5 reanalysis data for the period 1979-2014, while internal climate variability was preserved by incorporating 6-hourly anomalies from a single CMIP6 model (MPI-ESM1-HR).

The model was configured with a single domain of a 20-km spatial and 6-hour temporal resolution. It covers an area ranging from -115ºW to 40ºE in longitude, and 60ºN to 20ºS in latitude (Figure 1). Nevertheless, only data above 20°N was selected to perform the analysis, since the WRF parametrization used in this study shows especially positive results in subtropical and extratropical areas (Insua-Costa & Miguez-Macho, 2018; Insua-Costa et al., 2019). The year 2014 was considered as the study period, because it is qualified as a typical year since the dominant regional variability patterns, like the North Atlantic Oscillation and El Niño–Southern Oscillation, did not exhibit extreme phases (Fernández-Alvarez et al., 2023a). Also, this year has been used by Liu et al. (2018) for summer studies in the Asian region, specifically on China. Additionally, the following parameterizations were used: WSM6 microphysics scheme (Hong & Lim, 2006), Yonsei University planetary boundary layer scheme (Hong et al., 2006), Unified Noah land-surface model (Tewari et al., 2004), Revised MM5 surface layer scheme (Jiménez et al., 2012), RRTMG shortwave and longwave radiations scheme (Iacono et al., 2008) and Kain-Fritsch cumulus parametrization (Kain, 2004). Lastly, high resolution (30 s) geographical static data from the WRF preprocessing system (WRF Users Page, 2024) was used to perform the simulations.

https://doi.org/10.5194/egusphere-2025-1339
Preprint. Discussion started: 28 March 2025

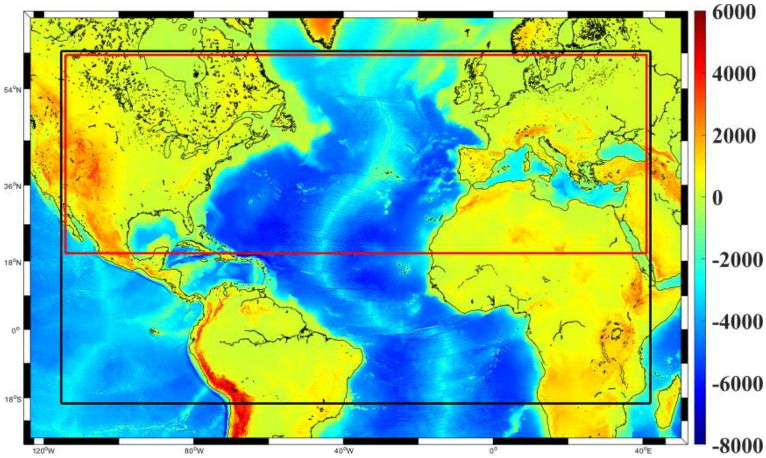

Figure 1. Topography and bathymetry (m) of the area where dynamical downscaling is performed. Black box represents the domain simulated with the WRF model, while red box is the area under study.

2.2. Dynamical downscaling methods

Two dynamic downscaling methods were performed, both using the WRF model with the previously described configuration. The only difference between them was whether the simulation was run continuously or as a series of short-term simulations, each initialized with a cold start. In the first method, a continuous simulation of the year 2014 was performed, corrected with spectral nudging for waves longer than 1000 km to minimize disruptions in the large-scale circulation within the regional model domain, caused by interactions between the model solution and the lateral boundary conditions (Fernández-Álvarez et al., 2023b). Additionally, the continuous simulation included a one-month spin-up period, starting on December 1, 2013, at 00:00 UTC, and was run on a single core. In the second method, the year 2014 was simulated using 365 independent daily runs, each preceded by a 12-hour spin-up period. Each short simulation required an adjustment period for the model to reach equilibrium, during which the outputs were discarded (Seck et al., 2015). As a result, each run lasted 36 hours, starting at 12:00 UTC on the previous day of interest. Moreover, these simulations were executed in parallel using 40 cores, significantly reducing the computational cost compared to the continuous simulation.

Let N represent the number of days to be simulated in a dynamical downscaling, T_D the time required to simulate one day, and S (in days) the spin-up period. For a continuous dynamical downscaling, the total simulation time T is calculated as $T_D(S + N)$. In a reinitialized downscaling approach, the total simulation time increases theoretically. For instance, with daily reinitialization and the same spin-up period, the total time required would be $T_D(SN + N)$. However, since each run is independent, they can be executed in parallel using multiple cores. If C is the number of cores, the total time becomes $T = T_D(SN + N)/C$. It is important to note that the spin-up period can vary between continuous and reinitialized simulations, affecting the time difference between the two methods. For example, simulating one year using 40 cores, with a spin-up period of one month (S_C) for the continuous run and 12 hours (S_R) for the reinitialized run, results in the computational time

https://doi.org/10.5194/egusphere-2025-1339
Preprint. Discussion started: 28 March 2025

of the reinitialized technique being about 3.46% of the continuous method. The higher spin-up period in the continuous run has minimal impact, since with a 12-hour value for S_C, the ratio increases slightly to 3.74%. If the spin-up period for the reinitialized simulation increases, the ratio rises significantly but remains below 100%. For S_R values of 1 day, 7 days, and 30 days, the ratios are approximately 5%, 18%, and 72%, respectively. Additionally, as N grows indefinitely, the ratio asymptotically approaches $(S_R + 1)/C$, which equals 3.75% under the given conditions, therefore the total length of the period to be simulated do not have a great impact. The most influential factor on the ratio between the computational times of the two methods is the number of cores. If only one core is used, continuous downscaling is faster, with the reinitialized-to-continuous time ratio at around 139%. Using two cores already benefits the reinitialized method, reducing the ratio to 69%. The ratio further decreases to below 50% with three cores, 10% with 15 cores, 5% with 25 cores, and so on. Lastly, it should be noted that in continuous simulations, nudging is often applied, and therefore the time required to simulate one day (T_D) would be higher than for reinitialized simulations.

Several variables were studied, to evaluate the performances of both simulation methods. Wind speed at 10 meters above surface (W10), air temperature at 2 meters above surface (T2), dew point temperature at 2 meters above surface (DPT2), and surface atmospheric pressure (PSFC) are instantaneous variables, obtained every 6 hours. Precipitation (RAIN) and surface shortwave solar flux downwards (RSDS), referred to as solar radiation, are accumulated variables, meaning the value obtained at a specific timestamp represents the accumulated value through the 6 hours preceding this same timestamp. All the aforementioned variables are direct outputs of the WRF simulations. Lastly, the integrated moisture vertical transport (IVT) was post-processed using the eastward (u) and northward (v) components of the wind, as well as the specific humidity (q), using the following equation:

$$\mathrm{IVT} = \sqrt{\left(\frac{1}{g}\int_{\Omega} \mathrm{qudp}\right)^2 + \left(\frac{1}{g}\int_{\Omega} \mathrm{qvdp}\right)^2} \tag{1}$$

where Ω refers to the atmospheric column ranging between 1000 and 300 hPa (Ratna et al., 2016), and g to gravitational acceleration.

2.3. Validation of the dynamical downscaling methods

The two dynamical downscaling techniques were performed using both reanalysis and climatic data, as complementary approaches. The simulations were firstly performed using data from the ERA5 reanalysis dataset with a 1º spatial resolution, being dynamically downscaled by the WRF model to reach a 20-km one. Thus, the outputs of the simulation were compared with the ERA5 data with a 0.25º spatial resolution. By using the same data type for both the dynamical downscaling and the validation, potential biases related to differences in data sources are minimized. Dynamical downscaling simulations were also conducted using data from the CMIP6 multi-model ensemble (Xu et al., 2021) at 1.25º spatial resolution to force the WRF model. The resulting outputs, dynamically downscaled at 20-km, were then compared with the original ERA5 data at

https://doi.org/10.5194/egusphere-2025-1339
Preprint. Discussion started: 28 March 2025

its native 0.25º resolution. In this case, it is necessary to consider that the datasets for dynamical downscaling and validation are from different sources which can introduce some bias. Nevertheless, it is a common approach when modelling future climate data: an historical period must also be modelled and compared with observational or reanalysis data, such as the ERA5 dataset. Models that closely align with observed data are deemed reliable for representing real-world conditions and are therefore well-suited for forecasting future atmospheric trends. To achieve the validation process, a bilinear interpolation of the output grid (WRF, 20-km) on the comparison one (ERA5, 0.25º) was performed. This way, the values of the several variables can be compared at the exact same grid points. Moreover, only the 6-hourly data from ERA5 and CMIP6 were used, for the year 2014, to coincide with the WRF outputs temporal resolution.

Several metrics were applied to validate the results of both simulation methods using ERA5 data as the validation dataset. First of all, the Overlapping Percentage (OP, Perkins et al., 2007), between the WRF outputs and the ERA5 data, was calculated at each grid point. It consists in computing the probability density function of each series of values, using a specified number of bins and increment between them. Then, the OP is calculated, at every one of the grid points, using the next equation:

$$\mathrm{OP}\ (\%) = 100 * \sum_{i=1}^{n} \mathrm{minimum}\left(Z_i^{WRF}, Z_i^{ERA5}\right) \tag{2}$$

where n is the number of bins, and Z_i is the frequency of occurrence of the variable's value corresponding to the bin (i), from the WRF or ERA5 dataset. This metric permits to compare the global distribution of the simulated and the reference values of a variable. The higher its value, the higher the resemblance between both datasets.

Another metric, the Normalized Root Mean Square Error (NRMSE) was used to validate the results of the dynamical downscaling processes at each grid point, following the next formula:

$$\mathrm{NRMSE}\ (\%) = \sqrt{\frac{\sum_{t=1}^{T}\left(x_t^{WRF} - x_t^{ERA}\right)^2}{T}} \Big/ \left(x_{max}^{ERA} - x_{min}^{ERA}\right) \tag{3}$$

where T is the number of time steps (1460 for the year 2014 with a 6-hour temporal resolution), x_t is the value of the variable at time step (t), from the WRF or ERA5 dataset, and x_{min}^{ERA} and x_{max}^{ERA} are the minimal and maximal values from the ERA data, considering all time steps, at the specific grid points. Basically, this metric is the Root Mean Square Error (RMSE) normalized by the amplitude of the ERA5 signal and permits to compare the instantaneous difference between the simulated and the reference values of a variable, meaning at each one of the time steps. The lower its value, the lesser the differences between both datasets.

https://doi.org/10.5194/egusphere-2025-1339
Preprint. Discussion started: 28 March 2025

In order to compare the results of the validation between the reinitialized and continuous dynamical downscaling processes, the difference between the metrics (OP and NRMSE) calculated for both of these methods was computed using the following formulas.

$$\Delta OP\ (\%) = OP^{Reinitialized} - OP^{Continuous} \tag{4}$$

$$\Delta NRMSE\ (\%) = NRMSE^{Continuous} - NRMSE^{Reinitialized} \tag{5}$$

Thus, for both of these metrics, a positive value of Δ indicates a more accurate dynamical downscaling using the reinitialized method, as well as a negative value of the continuous method. Additionally, the metrics of comparison were also averaged across the area under study according to the soil type. The soil type "Ocean" represents grid cells entirely covering ocean or sea areas, while "Coast" corresponds to cells that include both sea and land surfaces. For the remaining grid cells, areas with altitudes below 1000 m are categorized as "Land" whereas regions with altitudes above 1000 m are classified as "Mountain".

Lastly, for all the variables under study, Taylor diagrams (Taylor, 2001) were plotted, showing the standard deviation (STD, equation 6) of the reference and modelled data, as well as the Correlation Coefficient (CC, equation 7) between them, according to the soil type. The RMSE were not plotted, for better readability of the figures, and since similar information is already known with the NRMSE variable, described previously. The unit of the STD metric is the same as the one of the variables under study, while CC are expressed as number between 0 and 1, corresponding to percentages. Both these metrics permit, like the NRMSE, to perform an instantaneous comparison.

$$STD = \sqrt{\frac{\sum_{i=1}^{N}(x_i - \overline{x})^2}{N}} \tag{6}$$

$$CC = \frac{\sum_{i=1}^{N}\left(x_i^{WRF} - \overline{x^{WRF}}\right)\left(x_i^{ERA} - \overline{x^{ERA}}\right)}{\sqrt{\sum_{i=1}^{N}\left(x_i^{WRF} - \overline{x^{WRF}}\right)^2 \sum_{i=1}^{N}\left(x_i^{ERA} - \overline{x^{ERA}}\right)^2}} \tag{7}$$

In these equations, x_i represents the values of the variable for all grid points corresponding to the specific soil type, and all the time steps of the simulations (total of N values), while $\overline{x}$ is the average of these x_i values. The STD is computed for both the ERA5 validation data and the two WRF simulations, while the CC is calculated exclusively for the WRF simulations, with the ERA5 data included in the equation.

https://doi.org/10.5194/egusphere-2025-1339
Preprint. Discussion started: 28 March 2025

Only the OP was applied to validate the results of both downscaling methods when forced with CMIP6 data, as it serves as a climatic comparison metric. The other metrics described above are instantaneous and, therefore, cannot be applied to simulations using GCM data.

3. Results and Discussion

3.1. Dynamical downscaling forced with reanalysis data (ERA5)

3.1.1. Wind Speed at 10-meter height (W10)

The W10 OP and NRMSE distributions for both downscaling methods, as well as their differences for these two metrics, is shown in Figure 2. Climatologically, the continuous (Figure 2a) and reinitialized (Figure 2b) simulations exhibit very similar OP values. Over the sea, there is significant agreement with ERA5 data, with OP values generally exceeding 90%. Over land, OP values decrease slightly but still remain above 80% in most regions. Notably, values below 50% are mainly found in mountainous areas (see Figure 1). Similar OP values were obtained in the Gulf of Mexico (Costoya et al., 2019), and the eastern US coast (Costoya et al., 2020) using data from the Coordinated Regional Climate Downscaling Experiment (CORDEX), obtained through a continuous dynamical downscaling and compared with buoys data. Additionally, similar OP values were obtained in the waters of Atlantic Europe (Thomas et al., 2025) as well as the Canary Islands (Thomas et al., 2023) performing a daily-reinitialized dynamical downscaling (with a 12-hour spin-up period) from a CMIP6 multi-model ensemble, and comparing the results with ERA5 and buoys data. The differences in OP between the reinitialized and continuous simulations are highlighted in Figure 2c. Both over the sea and land, the two downscaling methods yield comparable results. However, in regions near Texas and Egypt, the continuous method performs better, showing a 10% increase. Similarly, mountainous areas show a slight advantage for the continuous simulation, with values approximately 10% higher. Table 1 presents the OP values averaged according to soil type, confirming the excellent performance over the sea for both simulations, with values around 94% and minimal variation (STD below 3%). Over land, the continuous and reinitialized simulations show similarly high OP values, though slightly lower at approximately 83% and with greater spatial variability (STD around 12%). In mountainous regions, the continuous simulation achieves better results (+2%) but remains lower overall (~64%) with significant variability (STD ~19%). Additionally, Table 1 provides details for coastal areas, which are not clearly visible in Figure 2. Both downscaling methods effectively model W10 in these areas, with OP values exceeding 80%. However, the continuous simulation yields slightly higher values (~85%, +3%) and better spatial consistency (STD ~10%, +1%).

Regarding NRMSE, which reflects the temporal consistency between simulated and reference data, the outcomes are very similar. Figures 2d and 2e illustrate the spatial distribution of this metric for the continuous and reinitialized simulations, respectively. The lowest NRMSE values, ranging from 5-10%, are observed in the Atlantic Ocean, while a slight increase is noted in the Gulf of Mexico, the Mediterranean, and the Black Sea (~10%). Comparable NRMSE values are found over land, except in mountainous regions where they exceed 25%. Figure 2f, depicting the NRMSE difference between the continuous and reinitialized simulations, indicates that the reinitialized simulation generally performs slightly better over the sea (+5%), as well as in areas near Egypt and Texas. Similar to the OP metric, the continuous simulation yields marginally better results in mountainous regions, particularly in the Alps, with NRMSE values about 15% higher. Table 1 supports these observations, showing slightly better results over the sea for the reinitialized simulation (~6%, +1%), with low variability for both downscaling methods (STD ~2%). Over land, the values are higher and very similar between the two approaches (~14%, STD ~8%). In mountainous regions, both methods yield relatively low values, but the continuous run performs slightly better (~28%, +1%) and displays more uniformity (STD ~22%, +1%). Finally, both simulations demonstrate good accuracy in coastal areas, with NRMSE values around 13% and a standard deviation of about 7%, comparable to those over land.

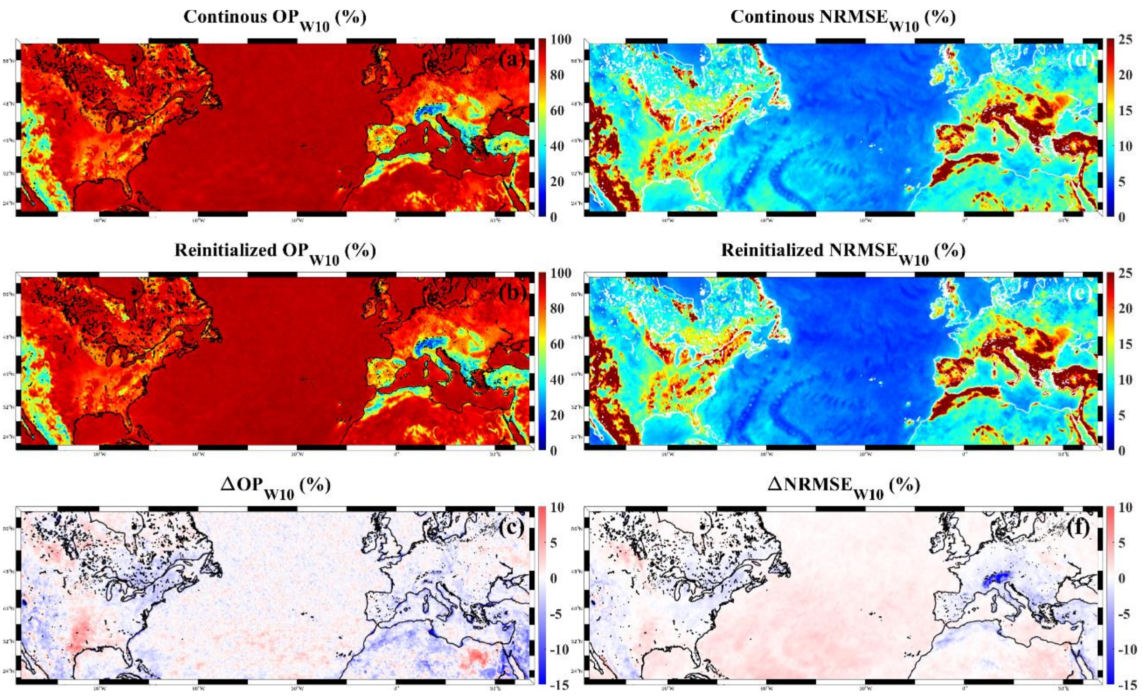

Figure 2. W10 variable: (left column) OP and (right column) NRMSE between WRF and ERA5 data for the (first row) continuous and (second row) reinitialized simulations, and (third row) differences between the two methods.

https://doi.org/10.5194/egusphere-2025-1339
Preprint. Discussion started: 28 March 2025

Table 1. W10 variable: OP and NRMSE between WRF and ERA5 for the continuous and reinitialized simulations, spatially averaged according to the soil type, and standard deviation.

	OP (%)		NRMSE (%)	
	Reinitialized	**Continuous**	**Reinitialized**	**Continuous**
Ocean	93.7 ± 2.6	93.8 ± 2.0	6.5 ± 2.2	7.5 ± 2.2
Coast	82.8 ± 11.1	85.5 ± 9.9	13.2 ± 7.3	12.6 ± 6.3
Land	83.1 ± 12.0	83.5 ± 11.7	13.9 ± 8.5	13.8 ± 7.9
Mountain	62.6 ± 18.9	64.2 ± 19.1	29.5 ± 23.1	28.2 ± 21.8

The CC and STD of the simulated W10 values based on soil type is shown in Figure 3. Over land and mountainous areas, the ERA5 reference data shows an STD of approximately 1.9 m/s, whereas the simulated values display a STD of about 2.1 m/s (+11%) for land and 2.4 m/s (+26%) for mountainous regions. The CC over land is approximately 0.80, while over mountains it drops to around 0.63. The results from both simulations are nearly identical. In coastal areas, the reference data has a STD close to 2.6 m/s, compared to 2.7 m/s (+4%) and 2.8 m/s (+8%) for the continuous and reinitialized simulations, respectively, with both showing a CC of 0.81. Over the sea, the reference data indicates an STD of around 3.7 m/s, whereas the continuous and reinitialized runs have STDs of approximately 3.8 m/s (+3%) and 3.9 m/s (+5%), respectively. However, the CC for the continuous method is about 0.93, slightly lower than the 0.95 observed for the reinitialized approach. Fernández-Alvarez et al. (2023b) used the WRF model to dynamically downscale data from a CMIP6 model (CESM2) through a continuous simulation. Their validation, comparing results with ERA5, showed relatively uniform values across the Atlantic Ocean. In a region like that of the present study, but extending southward to the Equator, they reported a sea surface CC of approximately 0.93, closely matching the value found in this study.

https://doi.org/10.5194/egusphere-2025-1339
Preprint. Discussion started: 28 March 2025

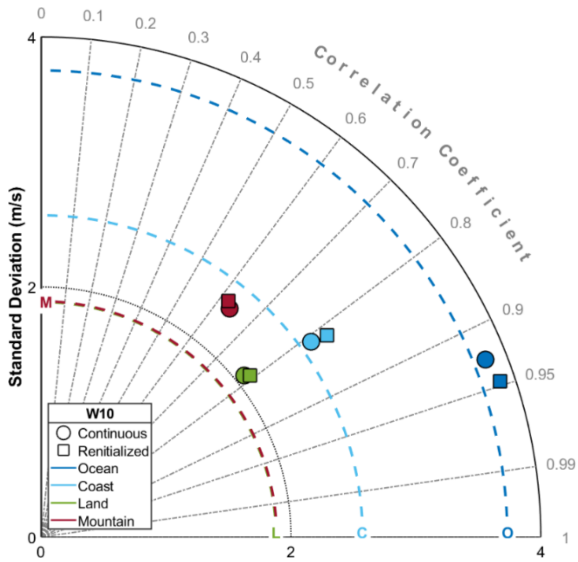

Figure 3. W10 variable: CC and STD for the continuous (circles) and reinitialized simulations (squares) according to the soil type. Colored dotted lines represent the STD of the reference data (ERA5).

3.1.2. Air Temperature at 2-meter height (T2)

Figure 4 presents the OP and NRMSE metrics for the T2 variable for both downscaling methods, along with the differences between the two methods. From a climatic perspective, the continuous (Figure 4a) and reinitialized (Figure 4b) simulations demonstrate consistently high OP values, exceeding 80% across the entire region. The values are notably elevated over the sea, often surpassing 90%, while they are slightly reduced over land. However, the continuous run appears to produce poorer outcomes in coastal zones, where the OP may drop to 50%, unlike the reinitialized simulation, which maintains strong continuity in values between the sea and land. Figure 4c illustrates the OP differences between the two downscaling methods, confirming this coastal discrepancy, as the reinitialized run shows up to 30% higher OP values. Over the sea, the methods generally yield similar outcomes, with the exception of areas west of North Africa, where the continuous run outperforms by 10%, and in the Hudson Bay, where the reinitialized method has a 10% advantage. On land, both approaches produce highly comparable results, aside from the Alps and North Africa, where the continuous run demonstrates a 10% improvement, and above Canada where its counterpart shows a similar increase. Table 2 corroborates that both downscaling methods deliver comparable results over the sea, with an average OP of about 93%. However, the reinitialized run demonstrates lower variability, with an STD of approximately 3%, which is 3% better than that of the continuous run. Over land and mountainous regions, both simulations yield slightly lower yet similar outcomes, with average OP values around 88% and STDs of 3%. In coastal areas, the reinitialized run achieves a consistent OP with a STD of around 4%, whereas the continuous run shows significantly poorer results, with a 9% decrease in OP and a 7% increase in STD, indicating greater variability.

The NRMSE distribution reveals a similar pattern. Both simulations show the best results over the sea, with values around 5%, except in the Hudson Bay for the continuous run (Figure 4d) and near the Greater Antilles for both downscaling methods (~10%). Over land, values are generally low (approximately 5%), except in regions like the Alps, North Africa, and the Rocky Mountains in the US, where they can reach up to 10%, especially in the reinitialized run (Figure 4e). Moreover, the continuous run exhibits higher NRMSE values in coastal regions, reaching up to 20% in certain areas, whereas the reinitialized method maintains greater continuity between sea and land. Jerez et al. (2020) obtained similar RMSE distribution in Europe, with values oscillating between 1.5 and 2.5 ºC performing a continuous dynamical downscaling with a one-month spin-up period and using the WRF model. Figure 4f, which shows the difference in NRMSE between the continuous and reinitialized runs, highlights the comparable results between both methods over the sea. The reinitialized run demonstrates improved performance in Canada and the Hudson Bay (+5%) and in coastal areas (up to +15%), while the continuous method shows a closer resemblance to the reference T2 (from ERA5) in the Rocky Mountains, the Alps, and North Africa (+5%). Table 2 shows that both simulations yield very similar NRMSE distributions over the sea, with values around 4% for the reinitialized run and 5% for the continuous run, accompanied by a 2% STD. Over land, both methods maintain a comparable NRMSE of approximately 5% and a similar STD, as well as in mountainous areas, with values around 6%, maintaining a similar STDs as observed in other terrain types. Finally, the reinitialized simulation achieves a NRMSE of about 5% in coastal regions, with a 2% STD, while the continuous run presents higher values, close to 9% in NRMSE and 4% in variability. Liu et al. (2018) explored T2 modelling using two dynamical downscaling approaches: daily reinitialized (with a 12-hour spin-up) and continuous (with spectral nudging) simulations. They used ERA-Interim data to drive the WRF model, and compared their results to 0.5º data from the National Meteorological Information Centre of the China Meteorological Administration. Their analysis, limited to land areas regardless of altitude, revealed spatially averaged RMSE values of 2.78 ºC and 3.17 ºC for the reinitialized and continuous approaches, respectively. In this study, focusing solely on land and mountainous regions, RMSE values of 2.54 ºC and 2.63 ºC were obtained for the same approaches. While both studies suggest that reinitialized dynamical downscaling provides more accurate T2 estimates over land, the present one globally shows better results, as well as lower difference between both techniques.

https://doi.org/10.5194/egusphere-2025-1339
Preprint. Discussion started: 28 March 2025

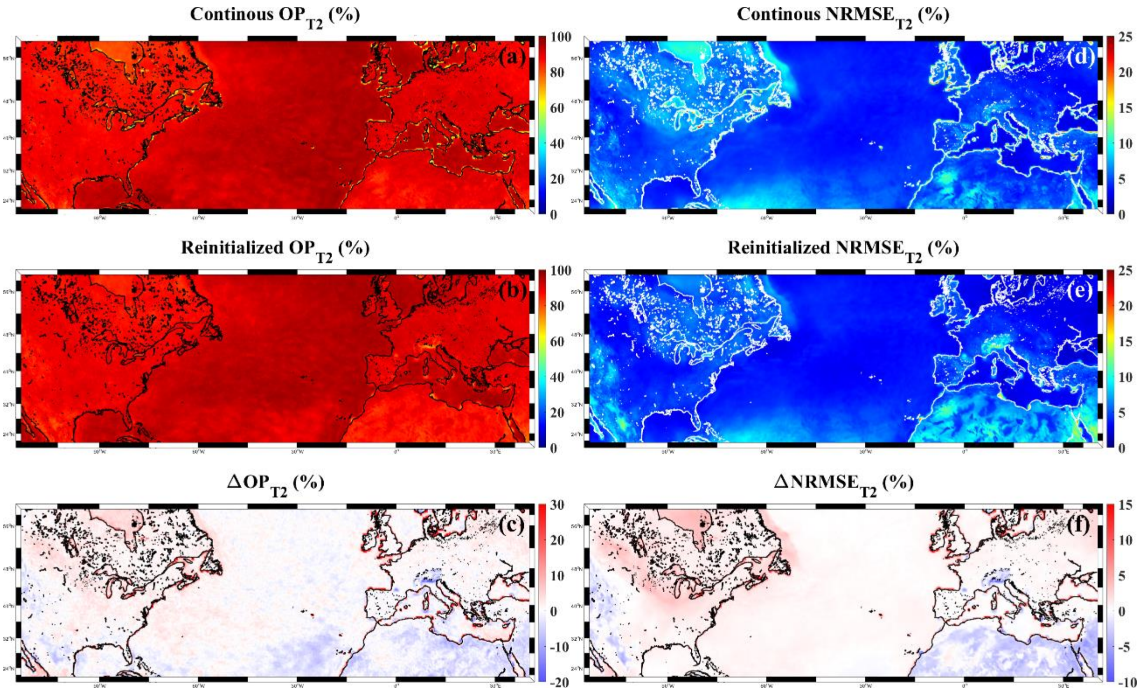

Figure 4. T2 variable: (left column) OP and (right column) NRMSE between WRF and ERA5 data for the (first row) continuous and (second row) reinitialized simulations, and (third row) differences between the two methods.

Table 2. T2 variable: OP and NRMSE between WRF and ERA5 for the continuous and reinitialized simulations, spatially averaged according to the soil type, and standard deviation.

	OP (%)		NRMSE (%)	
	Reinitialized	**Continuous**	**Reinitialized**	**Continuous**
Ocean	93.0 ± 2.7	92.3 ± 5.3	4.1 ± 1.5	4.8 ± 2.2
Coast	87.6 ± 3.7	79.3 ± 10.7	5.5 ± 2.2	8.7 ± 3.9
Land	88.0 ± 2.7	87.9 ± 2.5	5.2 ± 2.0	5.3 ± 1.4
Mountain	87.0 ± 3.0	87.6 ± 2.8	6.3 ± 2.1	5.6 ± 1.6

The CC and STD of simulated T2 values according to soil type is displayed in Figure 5. Over the sea, the ERA5 reference data has a STD of around 8.6 °C, with the reinitialized run showing 8.9 °C (+3%) and the continuous run being 0.1 °C higher (+5%). Both simulations have a comparable CC, slightly above 0.99. In mountainous regions, both runs also share a CC of 0.97. The STD for the reference data is 11.3 °C, while it is 11.2 °C (-1%) for the reinitialized run and 10.9 °C (-4%) for the continuous run. In coastal areas, the continuous run presents an STD of 14.5 °C (+6%), which aligns more closely with the reference data (13.7 °C) than the reinitialized run (14.6 °C, +7%). However, the reinitialized simulation exhibits a higher CC of 0.99, compared to 0.97 for the continuous run. Over land, both runs show a similar CC of 0.99. The STD in the reference data is 14.5 °C, while it measures 14.8 °C for the reinitialized run (+2%) and 15.4 °C for the continuous run (+6%). When analysing the average CC over land and mountainous regions, both techniques yield similar values of approximately 0.98. This aligns with Liu et al. (2018), who also reported comparable results between the two methods, though slightly lower, at around 0.90.

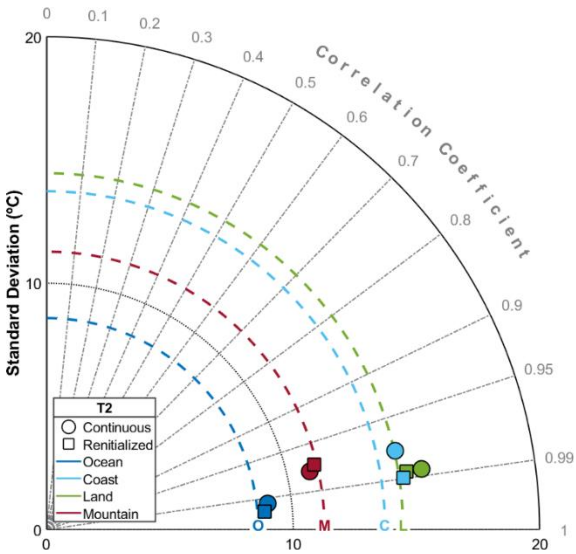

Figure 5. T2 variable: CC and STD for the continuous (circles) and reinitialized simulations (squares) according to the soil type. Colored dotted lines represent the STD of the reference data (ERA5).

3.1.3. Dew Point Temperature at 2-meter height (DPT2)

Figure 6 displays the OP and NRMSE metrics for the DPT2 variable for both downscaling methods, emphasizing the differences between the two methods. From a climate perspective, the continuous (Figure 6a) and reinitialized (Figure 6b) simulations consistently achieve high OP values, surpassing 80% across most of the region. However, the continuous simulation tends to show reduced performance in coastal areas, with OP values potentially dropping to 50%, unlike the reinitialized run, which maintains more consistent values between the sea and land. This coastal discrepancy is further highlighted in Figure 6c, where the reinitialized method shows up to 30% higher OP values. Over the sea, the reinitialized simulation typically performs better, with improvements of up to 10%. On land, both approaches yield similar results, except in North Africa, where the reinitialized run shows up to a 20% improvement, apart from its Mediterranean region, where the continuous run records a 10% increase in OP. This could be related to the fact that this variable depends on the relative humidity and evaporation and specifically, the Mediterranean is a very evaporative area (Gimeno et al., 2010), which is perhaps better reflected in continuous simulations (Liu et al., 2018). Near Mexico and Texas, the reinitialized simulation also shows a 10% improvement. According to Table 3, the reinitialized method generally produces superior results regardless of soil type, showing a 90% OP over the sea (+2%) and 88% over land and mountainous regions (+1%). While the standard deviation (STD) of the reinitialized method is 3% better over the sea, both techniques exhibit similar variability over land

https://doi.org/10.5194/egusphere-2025-1339
Preprint. Discussion started: 28 March 2025

and mountains. However, in coastal regions, the continuous simulation is notably less effective, with an OP of 76% (-12%) and a higher variability, indicated by an STD of 15% (+11%).

Regarding NRMSE, the reinitialized simulation (Figure 6d) generally shows marginally better outcomes, although both downscaling methods produce comparable results. Most regions display relatively low NRMSE values (~5%), except for certain areas such as the Rocky Mountains, the Alps, the coastal zones of Morocco and Algeria, and the vicinity of the Red Sea, where values reach around 10% and can peak at 25%. In the oceanic area west of North Africa, NRMSE values hover around 10% for the continuous run (Figure 6e) only. Figure 6f, which illustrates the differences in NRMSE between the two methods, confirms that the reinitialized simulation generally achieves better performance, with improvements between 5% and 10% across most of the domain and up to 15% in coastal regions. Table 3 further supports these observations. Both simulations yield similar results in mountainous areas, with an average NRMSE of approximately 8% and a STD of 3%. However, the reinitialized method achieves NRMSE values of 5% over the ocean and 6% over coastal and land areas, while the continuous method exhibits NRMSE values that are 2%, 4% and 1% higher in these regions, respectively. Variability over land is similar for both methods (STD ~ 3%), but the continuous simulation shows poorer performance over the ocean (+1% STD) and coastal regions (+2% STD), with variability values of 2% and 5%, respectively.

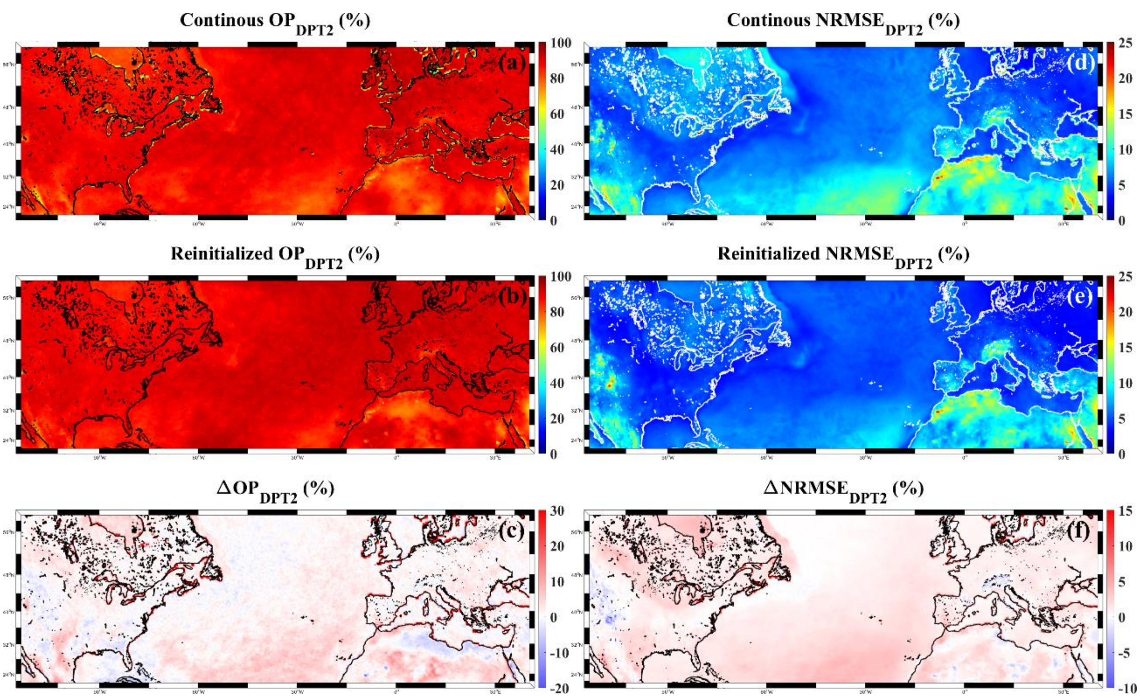

Figure 6. DPT2 variable: (left column) OP and (right column) NRMSE between WRF and ERA5 data for the (first row) continuous and (second row) reinitialized simulations, and (third row) differences between the two methods.

https://doi.org/10.5194/egusphere-2025-1339
Preprint. Discussion started: 28 March 2025

Table 3. DPT2 variable: OP and NRMSE between WRF and ERA5 for the continuous and reinitialized simulations, spatially averaged according to the soil type, and standard deviation.

	OP (%)		NRMSE (%)	
	Reinitialized	**Continuous**	**Reinitialized**	**Continuous**
Ocean	89.9 ± 3.0	87.6 ± 5.7	5.4 ± 1.2	7.0 ± 2.3
Coast	88.1 ± 4.2	76.0 ± 15.5	6.0 ± 2.8	9.9 ± 4.7
Land	88.3 ± 3.9	86.8 ± 4.5	6.2 ± 2.8	7.3 ± 2.9
Mountain	87.7 ± 3.8	86.9 ± 4.6	8.3 ± 2.7	8.5 ± 2.8

Figure 7 illustrates the CC and STD of simulated DPT2 values across different soil types. The reference data shows a STD of approximately 8.6 °C over both the sea and mountainous areas. Over the sea, the reinitialized and continuous simulations have slightly higher STDs, at 8.7 °C (+1%) and 8.8 °C (+2%), respectively. In mountainous regions, the reinitialized simulation records an STD of 8.8 °C (+2%), while the continuous one shows 8.5 °C (-1%). Both simulations yield similar CC values, about 0.99 over the sea and 0.93 in mountainous zones. Over land, the reinitialized run records an STD of 11.5 °C (+5%), compared to 11.0 °C for the reference data and 11.8 °C for the continuous simulation (+7%), with both achieving a CC of approximately 0.97. In coastal areas, both simulations have an STD of about 13.7 °C, which is 0.5 °C higher than the reference (+4%). The reinitialized simulation maintains a CC close to 0.99, while the continuous simulation lags slightly with a CC that is 0.04 points lower. Liu et al. (2018) also obtained similar CC values for the relative humidity between both dynamical downscaling techniques, though quite lower (around 0.65) across all land types in China.

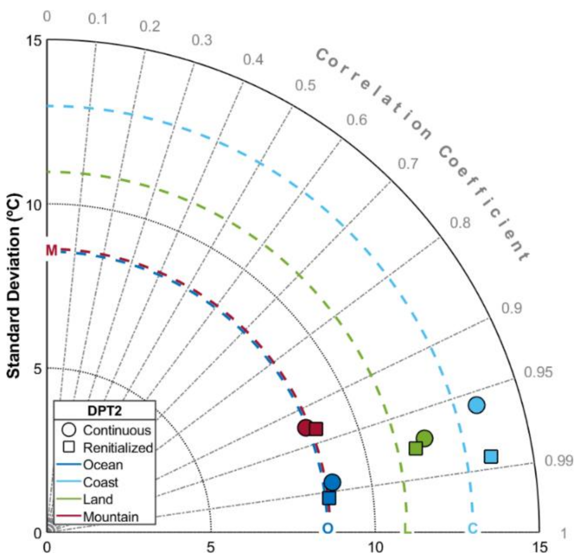

Figure 7. DPT2 variable: CC and STD for the continuous (circles) and reinitialized (squares) simulations according to the soil type. Colored dotted lines represent the STD of the reference data (ERA5).

3.1.4. Accumulated Precipitation (RAIN)

Figure 8 presents the OP and NRMSE distributions for the RAIN variable for both downscaling approaches, highlighting the differences between the two methods. From a climatic perspective, both the continuous (Figure 8a) and reinitialized (Figure 8b) simulations consistently exhibit substantial OP values, exceeding 70% across the entire region. Notably, OP values surpass 90% in North Africa, while the lowest values, around 70%, are found in the western Atlantic Ocean. The rest of the region generally shows OP values above 80%. Figure 8c, which illustrates the differences in OP values between reinitialized and continuous runs, indicates that the continuous simulation generally models the RAIN variable more accurately over the sea, with results up to 10% higher, and in Eastern Europe, with an increase of about 5%. On the other hand, the reinitialized simulation performs better along the Gulf of Mexico's coastal areas, with OP values approximately 5% higher. Across most of the domain, both methods show minimal differences, particularly in North Africa. These findings are supported by Table 4, which shows average OP values of 85%, 90%, 93%, and 92% over the sea, coastal regions, land, and mountains, respectively, regardless of the simulation type. In terms of STD, values range between 4% and 5% for the latter three terrain types, while they fluctuate between 6% and 7% over the sea.

Regarding NRMSE, the spatial distribution for the continuous (Figure 8d) and reinitialized (Figure 8e) simulations appears rather irregular. Most regions exhibit values between 5% and 15%, with localized peaks reaching up to 25%, particularly in northeastern Africa. Jerez et al. (2020) obtained a similar RMSE distribution in Europe, though with different magnitude since they computed the daily-accumulated precipitation. The highest variability is observed in coastal areas of the Adriatic Sea. Figure 8f, which depicts the NRMSE differences between the two downscaling methods, indicates that the reinitialized simulation achieves marginally better results across the study area, generally outperforming the continuous run by a few percentage points, with an increase up to 20% in the northeast corner of Africa. Table 4 corroborates these observations, showing that the reinitialized simulation performs slightly better (+1%) over the ocean (7%), land (8%), and mountains (9%). Both simulations display similar variability over the ocean (STD ~ 3%) and mountains (STD ~ 5%). However, over land, the continuous simulation exhibits greater heterogeneity, with a 5% higher STD, reaching 10%. Finally, in coastal areas, both methods report comparable NRMSE values of approximately 8%, with STDs around 3%. Liu et al. (2018), analysing the daily-accumulated precipitation above lands in China, obtained similar RMSE values around 11.0 and 11.6 mm for the continuous and reinitialized runs, respectively, quite worse than the 1.45 and 1.38 mm obtained in the present study for the 6-hour accumulated precipitation.

https://doi.org/10.5194/egusphere-2025-1339
Preprint. Discussion started: 28 March 2025

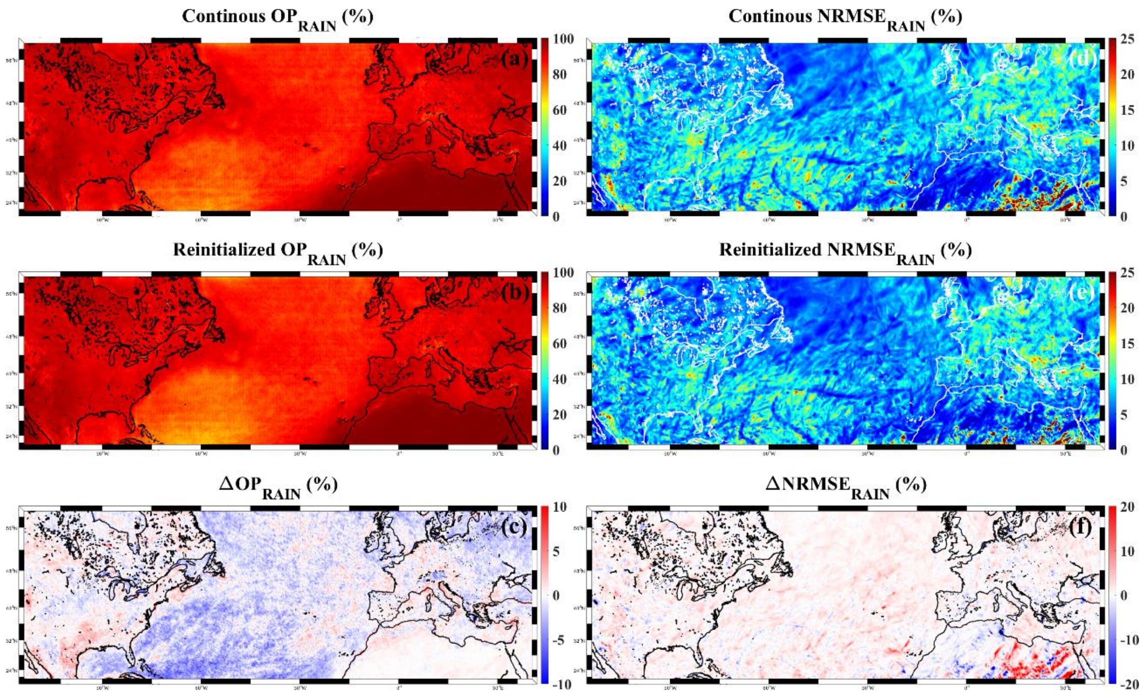

Figure 8. RAIN variable: (left column) OP and (right column) NRMSE between WRF and ERA5 data for the (first row) continuous and (second row) reinitialized simulations, and (third row) differences between the two methods.

Table 4. RAIN variable: OP and NRMSE between WRF and ERA5 for the continuous and reinitialized simulations, spatially averaged according to the soil type, and standard deviation.

	OP (%)		NRMSE (%)	
	Reinitialized	**Continuous**	**Reinitialized**	**Continuous**
Ocean	84.4 ± 6.7	85.5 ± 6.2	7.0 ± 2.8	7.7 ± 2.8
Coast	89.8 ± 4.4	89.5 ± 4.8	7.7 ± 3.6	7.7 ± 3.2
Land	92.9 ± 4.5	92.9 ± 4.4	8.0 ± 5.2	8.8 ± 9.8
Mountain	91.9 ± 4.7	92.0 ± 4.5	8.8 ± 4.8	9.4 ± 4.6

Figure 9 displays the CC and STD of simulated RAIN values across different soil types. While the continuous run shows STDs more closely aligned with the reference data, the reinitialized simulation achieves higher CC values. The ERA5 reference data reports STDs of 1.4 mm for mountains, 1.6 mm for land, 2.0 mm for coastal areas, and 2.2 mm over the sea. In comparison, the continuous simulation shows STDs of 2.0 mm (+43%), 2.1 mm (+31%), 2.2 mm (+10%), and 2.5 mm (+14%) for these areas, respectively. The reinitialized run presents higher STDs of 2.1 mm (+50%), 2.3 mm (+44%), 2.6 mm (+30%), and 2.9 mm (+32%) for the same soil types. Despite this, the reinitialized approach achieves better CC values, with 0.61 over mountains, 0.67 over land, 0.70 in coastal areas, and 0.71 over the ocean, while the continuous run records CC values of 0.53, 0.58, 0.63, and 0.60 for the respective regions. In China, Liu et al. (2018) reported CC values over land and

https://doi.org/10.5194/egusphere-2025-1339
Preprint. Discussion started: 28 March 2025

mountains of 0.43 for continuous and 0.12 for reinitialized downscaling. In contrast, the present analysis shows higher values of approximately 0.57 and 0.65, respectively, with a smaller difference between both methods and improved correlation, especially for the reinitialized run, which shows the best value. Additionally, Lo et al. (2008) reported CC values for daily-accumulated precipitation in the US, ranging globally from 0.30 to 0.80, with highly similar results for both continuous and reinitialized dynamical downscaling methods. The average values obtained in the present study fall within this range.

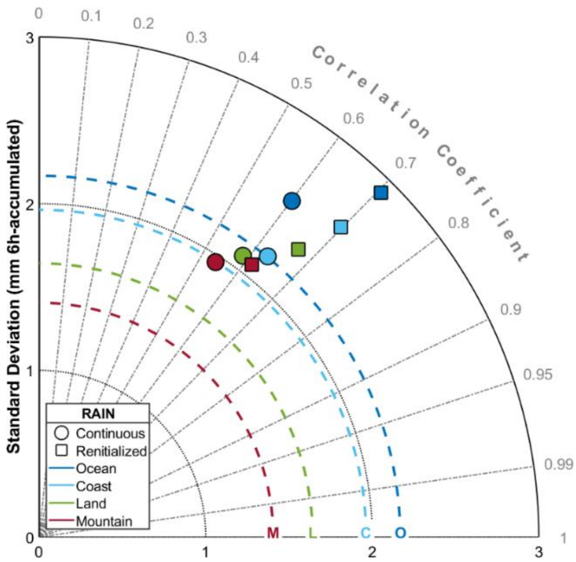

Figure 9. RAIN variable: CC and STD for the continuous (circles) and reinitialized (squares) simulations according to the soil type. Colored dotted lines represent the STD of the reference data (ERA5).

3.1.5. Surface Atmospheric Pressure (PSFC)

Figure 10 illustrates the OP and NRMSE distributions for the PSFC variable for the two downscaling methods, emphasizing the differences between the two methods. From a climatic perspective, both the continuous (Figure 10a) and reinitialized (Figure 10b) simulations demonstrate a comparable spatial distribution of OP values across the region of interest. On a broader scale, the OP exceeds 80%, reaching up to 90% over the ocean. However, mountainous regions (as indicated in Figure 1) distinctly show lower OP values, dropping below 50%. Figure 10c further indicates minimal variation between the two downscaling methods, with differences not exceeding a 5% increase for either approach. These observations are corroborated by Table 5, which shows that the average OP is nearly identical for both simulations: 89% over the ocean, 80% in coastal areas, 83% over land, and 60% in mountainous regions. The standard deviations for these areas are 4%, 15%, 13%, and 27%, respectively, suggesting limited variability only over the ocean.

https://doi.org/10.5194/egusphere-2025-1339
Preprint. Discussion started: 28 March 2025

The NRMSE distribution follows a similar trend for both the continuous (Figure 10d) and reinitialized (Figure 10e) simulations. Values remain below 5% across most of the region but increase to over 25% in mountainous areas. Figure 10f highlights the minor differences between the downscaling techniques, demonstrating their overall similarity. However, the reinitialized simulation shows slightly improved NRMSE values over the Atlantic Ocean and marginally higher values in regions like North Africa, the Mediterranean, and the Gulf of Mexico. Table 5 confirms these findings, indicating comparable results based on soil type: approximately 2% over the ocean (STD ~ 2%), 6% in coastal areas (STD ~ 9%), 5% over land (STD ~ 7%), and 19% in mountainous areas (STD ~ 21%). Lo et al. (2008), using the WRF model, performed several kinds of dynamical downscaling for a one-year period in the US, among them a continuous and a weekly-reinitialized one. Their results also show that both methods yield similar RMSE values for PSFC, around 5 hPa. Similarly, Pan et al. (1999) demonstrated the high similarity between continuous and daily-reinitialized dynamical downscaling techniques when analysing PSFC.

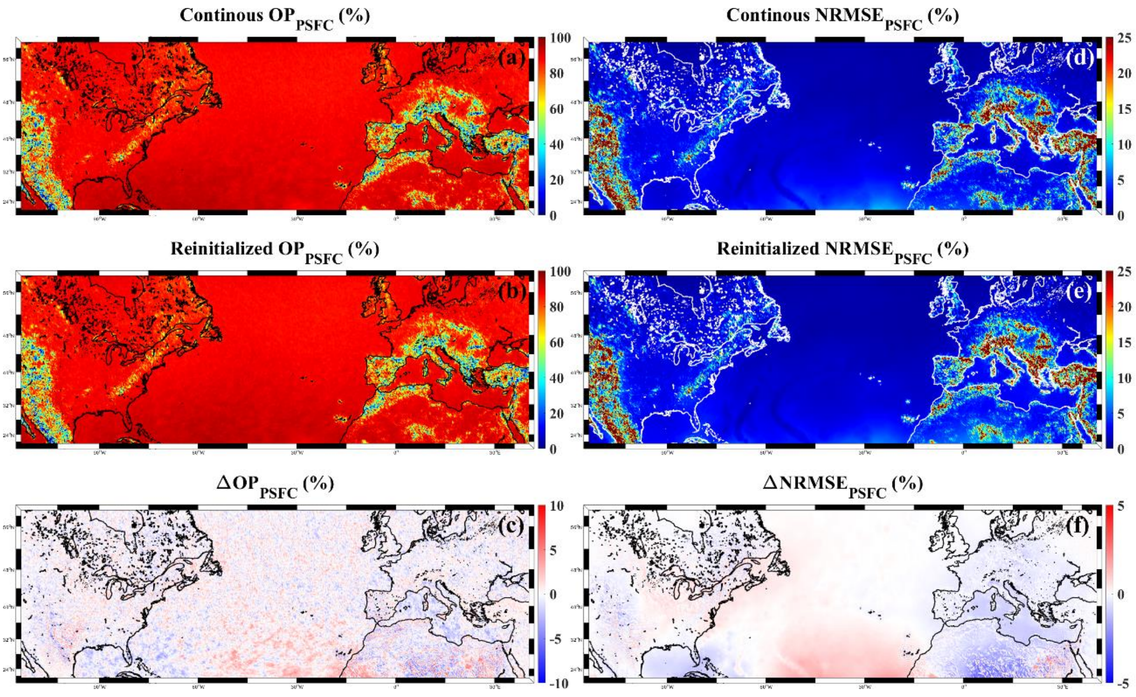

Figure 10. PSFC variable: (left column) OP and (right column) NRMSE between WRF and ERA5 data for the (first row) continuous and (second row) reinitialized simulations, and (third row) differences between the two methods.

https://doi.org/10.5194/egusphere-2025-1339
Preprint. Discussion started: 28 March 2025

Table 5. PSFC variable: OP and NRMSE between WRF and ERA5 for the continuous and reinitialized simulations, spatially averaged according to the soil type, and standard deviation.

	OP (%)		NRMSE (%)	
	Reinitialized	**Continuous**	**Reinitialized**	**Continuous**
Ocean	89.2 ± 3.7	89.1 ± 3.7	2.2 ± 1.7	2.3 ± 1.8
Coast	80.3 ± 15.0	80.2 ± 15.2	5.9 ± 9.3	5.9 ± 9.3
Land	83.0 ± 12.8	82.9 ± 12.9	5.4 ± 7.0	5.2 ± 7.0
Mountain	60.1 ± 27.3	60.0 ± 27.4	19.2 ± 20.7	19.0 ± 20.8

Finally, Figure 11 illustrates the CC and STD of simulated PSFC values across various soil types. The results show strong agreement with the reference data (ERA5), with CC values of approximately 0.99 for both simulations across all soil types. Over the ocean, the reference data presents a STD of 9.9 hPa, which is 0.1 hPa (-1%) and 0.2 hPa (-2%) lower for the reinitialized and continuous simulations, respectively. In coastal regions, the STD for the reference data is 22.3 hPa, with the reinitialized and continuous simulations showing an increase of 0.3 hPa (+1%) and 0.2 hPa (+1%), respectively. Over land, the reference data's STD is 29.1 hPa, with both simulations exhibiting a marginal increase of 0.1 hPa (< 1%). Such increase is observed in mountainous areas (< 1%), where the reference data indicates an STD of 48.5 hPa.

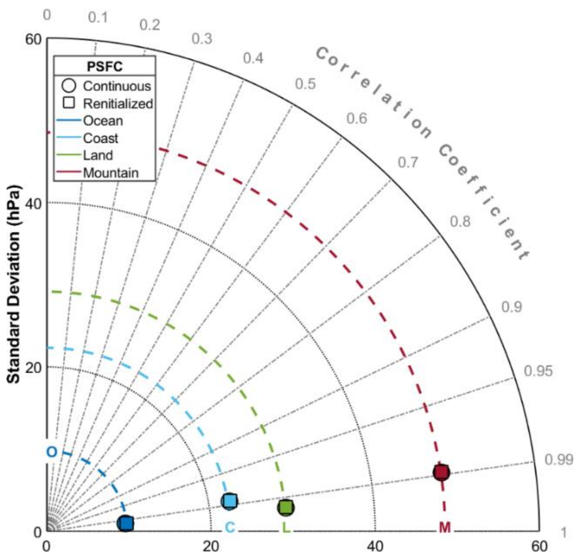

Figure 11. PSFC variable: CC and STD for the continuous (circles) and reinitialized (squares) simulations according to the soil type. Colored dotted lines represent the STD of the reference data (ERA5).

https://doi.org/10.5194/egusphere-2025-1339
Preprint. Discussion started: 28 March 2025

3.1.6. Accumulated Surface Short-Wave Solar Flux Downwards (RSDS)

The OP and NRMSE distributions for the RSDS variable for the two downscaling approaches is displayed in Figure 12, highlighting the differences between the two methods. From a climatic perspective, both the continuous (Figure 12a) and reinitialized (Figure 12b) simulations exhibit a similar pattern. Values remain fairly consistent across the study area, ranging between 70% and 80% for OP. The highest values are observed in North America and the Atlantic Ocean, while they tend to be slightly lower over Europe, and notably lower in North Africa, particularly in the reinitialized run. Comparable OP values derived from continuous dynamical downscaling and compared with ERA5 were reported in the US and its eastern coast (Costoya et al., 2023), as well as in the western Iberian Peninsula (Costoya et al., 2022) using CORDEX data. Figure 12c illustrates the difference in OP between the two simulations, showing comparable results in North America and the western Atlantic, while the continuous simulation exhibits superior values in the eastern region (+5%) and over Europe and North Africa (+10%). Table 6 corroborates the superior performance of the continuous simulation across various soil types. It reports 3% higher values over the ocean (85%), in coastal zones (86%), and over land (83%), and 2% higher in mountainous regions (83%) compared to the reinitialized run. Additionally, the continuous simulation demonstrates reduced variability, except over the sea, where both show a standard deviation of 4%. On land, as well as in coastal and mountainous regions, the variability is around 4%, which is 2% better than in the reinitialized simulation. These results might indicate that convection is better modelled in the continuous simulation.

Regarding NRMSE, the results show some differences. Although both the continuous (Figure 12d) and reinitialized (Figure 12f) simulations present similar distributions, the lowest values (~5%) are observed in the western part of North America and North Africa. These values increase in the Atlantic Ocean, peaking at approximately 10%, particularly in the reinitialized simulation, while the highest values (~15%) appear in Europe and the eastern part of North America. Figure 12f indicates that differences in NRMSE between the two runs are minimal over land, but the continuous simulation generally yields better outcomes over the ocean, notably in areas such as Hudson Bay, the Gulf of Mexico, and the Atlantic Ocean. Table 6 supports these observations. Both simulations exhibit similar results over land (9%, STD ~3%) and in mountainous regions (8%, STD ~2%). However, over the ocean and in coastal regions, the continuous simulation shows slightly better performance (9% and 8%, respectively), outperforming the reinitialized run by 1%, while maintaining comparable variability (STD ~2% and 1%, respectively).

https://doi.org/10.5194/egusphere-2025-1339
Preprint. Discussion started: 28 March 2025

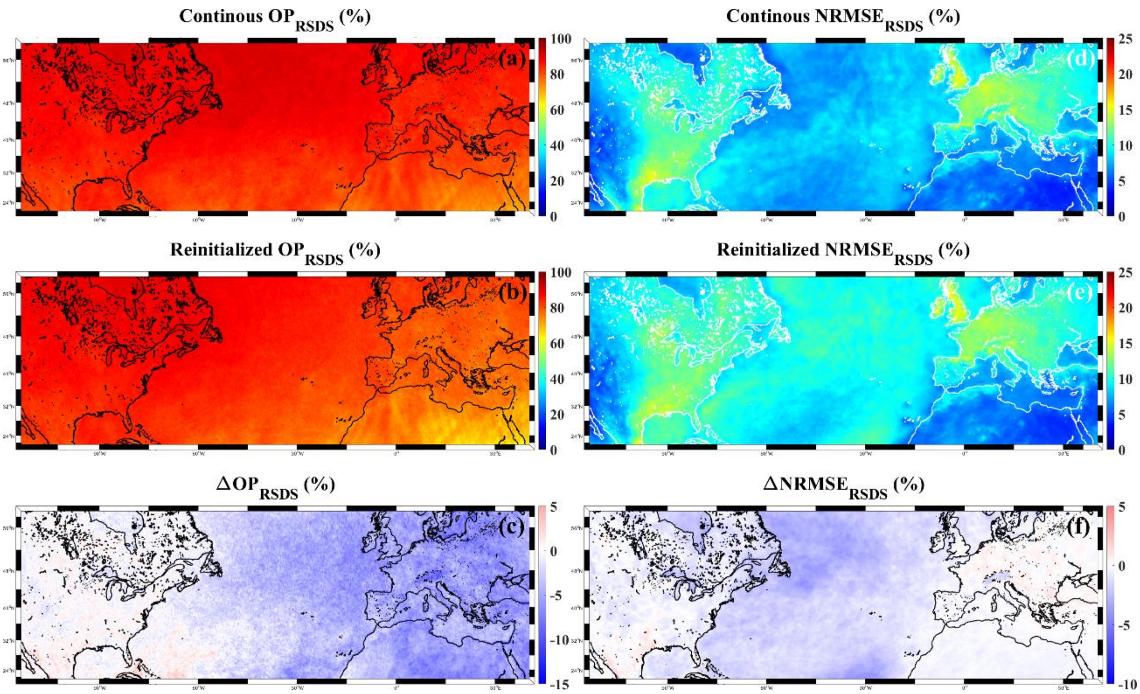

Figure 12. RSDS variable: (left column) OP and (right column) NRMSE between WRF and ERA5 data for the (first row) continuous and (second row) reinitialized simulations, and (third row) differences between the two methods.

Table 6. RSDS variable: OP and NRMSE between WRF and ERA5 for the continuous and reinitialized simulations, spatially averaged according to the soil type, and standard deviation.

	OP (%)		NRMSE (%)	
	Reinitialized	**Continuous**	**Reinitialized**	**Continuous**
Ocean	82.4 ± 4.0	85.3 ± 3.9	9.3 ± 1.4	7.8 ± 1.2
Coast	83.0 ± 5.6	85.8 ± 3.9	9.6 ± 2.0	8.8 ± 2.0
Land	80.3 ± 6.5	83.3 ± 4.5	9.3 ± 2.7	9.0 ± 2.7
Mountain	81.2 ± 5.7	83.4 ± 3.6	7.8 ± 1.8	7.5 ± 1.9

Figure 13 presents the CC and STD of simulated RSDS values across different soil types. The reference dataset (ERA5) shows a STD of 218 W/m² in coastal regions, while the continuous and reinitialized runs have higher STDs of 246 W/m² (+17%) and 251 W/m² (+20%), respectively. Both simulations achieve a similar CC of 0.97. Over the ocean, the continuous and reinitialized runs report STDs of 258 W/m² (+12%) and 259 W/m² (+12%), compared to 231 W/m² for the reference data. The continuous run has a slightly higher CC at 0.98, compared to 0.97 for the reinitialized run. On land, the reference data's STD is 239 W/m², with the continuous and reinitialized runs showing increases of 29 W/m² (+12%) and 31 W/m² (+13%), respectively, and CC values of 0.98 and 0.97. In mountainous regions, the continuous run records a STD of 287 W/m² (+28 W/m², +11%), while the reinitialized run has 289 W/m² (+30 W/m², +12%), both demonstrating a CC of 0.98.

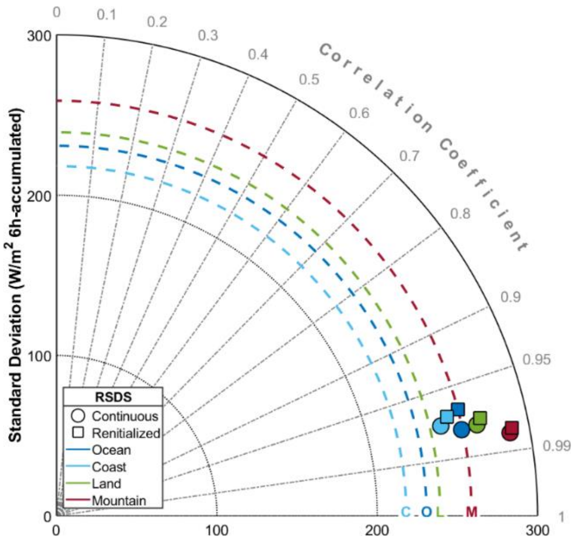

Figure 13. RSDS variable: CC and STD for the continuous (circles) and reinitialized (squares) simulations according to the soil type. Colored dotted lines represent the STD of the reference data (ERA5).

3.1.7. Integrated Moisture Vertical Transport (IVT)

Figure 14 illustrates the distributions of OP and NRMSE for the IVT variable for the two downscaling methods, emphasizing the differences between the two methods. From a climate analysis perspective, both continuous (Figure 14a) and reinitialized (Figure 14b) simulations yield highly similar outcomes, with OP values consistently near 90% across the studied region. However, the results appear marginally better (by a few percentage points) over land compared to the ocean. This observation is supported by Figure 14c, which indicates that the differences between the simulations are negligible. Table 7 corroborates these findings: the average OP values are approximately 88% over the ocean (STD ~ 2%), 90% in coastal zones (STD ~ 2%), and 91% over land and mountainous regions, with corresponding STDs of about 2% and 3%.

The NRMSE results, however, show some variation. While both continuous (Figure 14d) and reinitialized (Figure 14e) simulations present comparable distributions, the lowest NRMSE values (~ 5%) are predominantly observed over the ocean, North Africa, Atlantic Europe, and Canada. In contrast, the highest NRMSE values, reaching around 10%, are concentrated in the Rocky Mountains and Central Europe, particularly the Alps. Figure 14f highlights that the reinitialized simulation produces marginally improved NRMSE values, up to 5% lower in most regions, particularly over the Atlantic Ocean and North Africa. On the other hand, Central Europe shows slightly better results from the continuous simulation, probably due to the better accuracy of this method for modelling humidity transport in areas of complex orography. Table 7 reaffirms these findings, indicating average NRMSE values of 4% in coastal and land areas, and around 6% in mountainous regions, with STDs of 2%, 1%, and 2%, respectively, regardless the downscaling method. On the contrary, over the ocean, although

https://doi.org/10.5194/egusphere-2025-1339
Preprint. Discussion started: 28 March 2025

both simulations share an STD of approximately 1%, the continuous run shows a slight increase (+1%) in NRMSE, yielding a value of 5%.

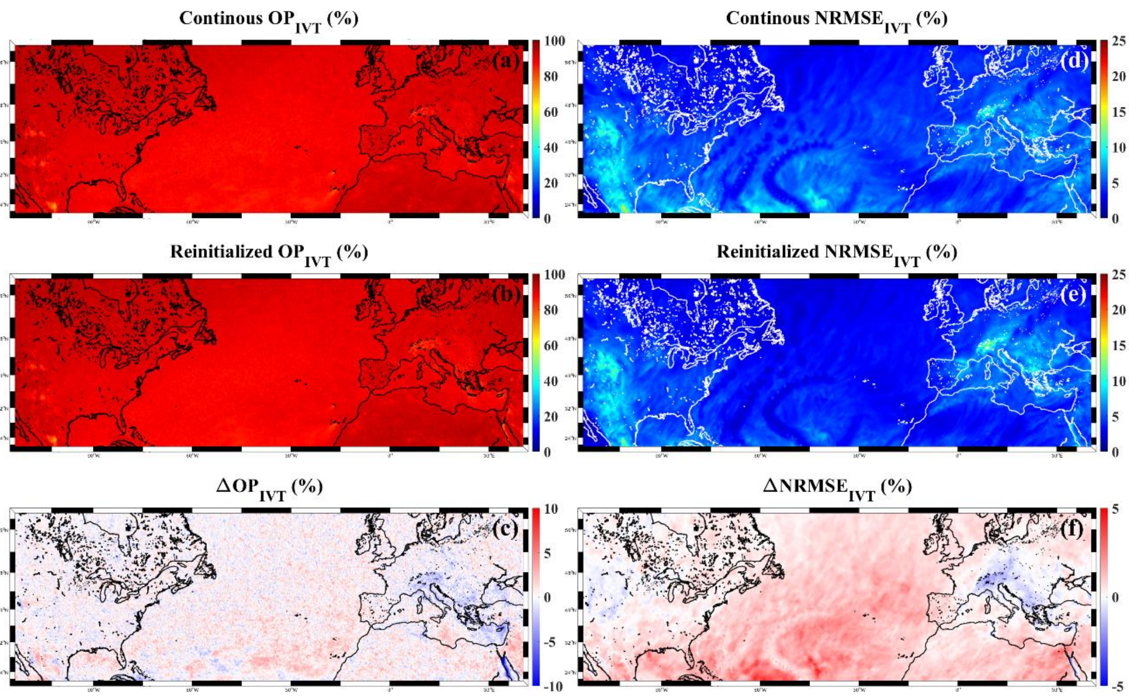

Figure 14. IVT variable: (left column) OP and (right column) NRMSE between WRF and ERA5 data for the (first row) continuous and (second row) reinitialized simulations, and (third row) differences between the two methods.

Table 7. IVT variable: OP and NRMSE between WRF and ERA5 for the continuous and reinitialized simulations, spatially averaged according to the soil type, and standard deviation.

	OP (%)		NRMSE (%)	
	Reinitialized	**Continuous**	**Reinitialized**	**Continuous**
Ocean	88.6 ± 1.9	88.3 ± 2.0	3.6 ± 1.3	4.7 ± 1.6
Coast	90.3 ± 2.4	90.5 ± 2.1	4.0 ± 1.7	4.3 ± 1.7
Land	91.3 ± 2.0	91.2 ± 1.9	4.2 ± 1.4	4.6 ± 1.4
Mountain	90.7 ± 3.0	90.6 ± 3.1	6.4 ± 2.0	6.6 ± 2.0

Figure 15 compares the CC and STD of simulated IVT values across various soil types. The reference dataset (ERA5) shows the lowest STD in mountainous areas, about 70 kg/m/s, compared to 69 kg/m/s (-1%) for the reinitialized run and 67 kg/m/s (-4%) for the continuous one. The reinitialized simulation achieves a CC of 0.90, slightly higher than the 0.89 seen in the continuous run. Over land, the reference data has a STD of 108 kg/m/s, while the continuous and reinitialized runs show values 2 kg/m/s (+2%) and 4 kg/m/s (+4%) higher, with CCs of 0.95 and 0.96, respectively. In coastal regions, the STDs are

https://doi.org/10.5194/egusphere-2025-1339
Preprint. Discussion started: 28 March 2025

128 kg/m/s (+4%) and 127 kg/m/s (+3%) for the reinitialized and continuous runs, compared to 123 kg/m/s for the reference data. The reinitialized run shows a slight advantage with a CC of 0.97, compared to 0.96 for the continuous one. Over the ocean, the reference dataset's STD is 158 kg/m/s, with the continuous and reinitialized runs having increases of 3 kg/m/s (+2%) and 4 kg/m/s (+3%), and CCs of 0.95 and 0.97, respectively.

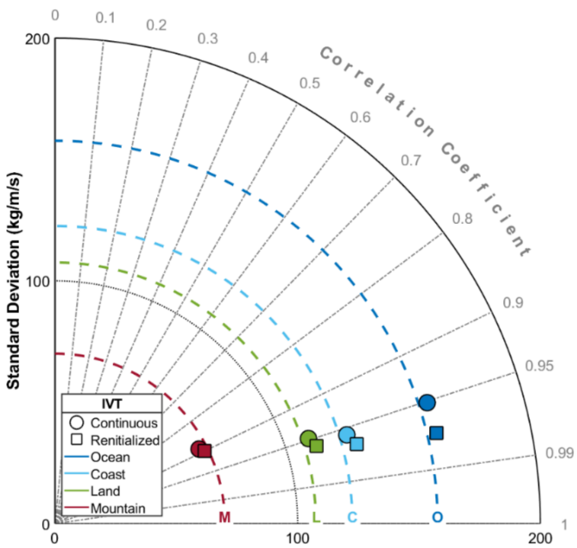

Figure 15. IVT variable: CC and STD for the continuous (circles) and reinitialized (squares) simulations according to the soil type. Colored dotted lines represent the STD of the reference data (ERA5).

3.2 Dynamical downscaling forced with GCM data (CMIP6)

When forcing the WRF model with CMIP6 data, the outputs from both dynamical downscaling techniques are also highly consistent. Table 8 shows the average OP between the modelled data and ERA5 at 0.25º, along with the STD of the OP, for each of the seven atmospheric variables analysed and across all soil types. Additionally, Figures A1 to A7 from the Appendix section illustrate the distribution of OP of all atmospheric variables variable for the two downscaling methods, as well as the differences between both techniques.

https://doi.org/10.5194/egusphere-2025-1339
Preprint. Discussion started: 28 March 2025

Table 8. Average OP (%) and associated STD (%) for the all the atmospheric variables and soil types, considering the CMIP6-driven continuous (reinitialized) technique. If there is no value between parenthesis, both techniques result in the same value.

		W10	T2	DPT2	RAIN	PSFC	RSDS	IVT
Ocean	OP (%)	91 (90)	83	82	84	83	86 (83)	86
	STD (%)	± 3	± 6	± 6	± 7	± 3	± 4	± 3
Coast	OP (%)	82 (81)	83 (81)	82 (80)	89 (88)	78	86 (83)	87
	STD (%)	± 11	± 5	± 6	± 5	± 14	± 4 (6)	± 3
Land	OP (%)	82 (79)	85 (82)	82 (78)	92 (91)	80	83 (80)	88
	STD (%)	± 13	± 3	± 5	± 5	± 11	± 4 (7)	± 3
Mountain	OP (%)	62 (58)	86 (85)	82 (79)	91	60	84 (82)	89
	STD (%)	± 20	± 3	± 6	± 4	± 26	± 4 (6)	± 3

Above the ocean, as shown in Figure 16, both dynamical downscaling techniques result in particularly similar values, with differences in average OPs values remaining below 1% for all variables except RSDS, which shows a difference of 3%. All OPs are above the 80%.

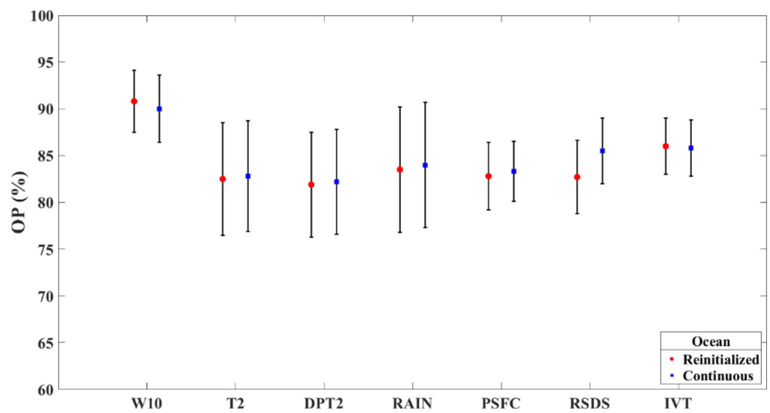

Figure 16. Average OP for the reinitialized (red circles) and continuous (blue squares) simulations, and standard deviations (black lines), over ocean areas.

When using CMIP6 data instead of ERA5 to drive the WRF model, a global decrease in OP values is observed in oceanic areas: 3% for W10, 10% for T2, 8% (reinitialized) and 5% (continuous) for DPT2, 1% for RAIN, 6% for PSFC, and 2% for IVT, with no changes for RSDS. In terms of STDs, overall values remain similar, with increases of 1% for W10 and IVT (in both downscaling techniques) and around 3% for T2 and DPT2 (only in the reinitialized simulation).

https://doi.org/10.5194/egusphere-2025-1339
Preprint. Discussion started: 28 March 2025

Figure 17 shows the average OP over coastal areas for each of the seven atmospheric variables analysed, along with their respective STDs. Both dynamical downscaling techniques produce similar results, with differences falling within the range of the STDs for all variables. The only notable difference is a 3% higher OP and 2% lower STD for RSDS in the continuous method, indicating a better correlation with the reference data and a slightly greater stability for this variable using that method (Table 8). All OPs are above or close to 80%.

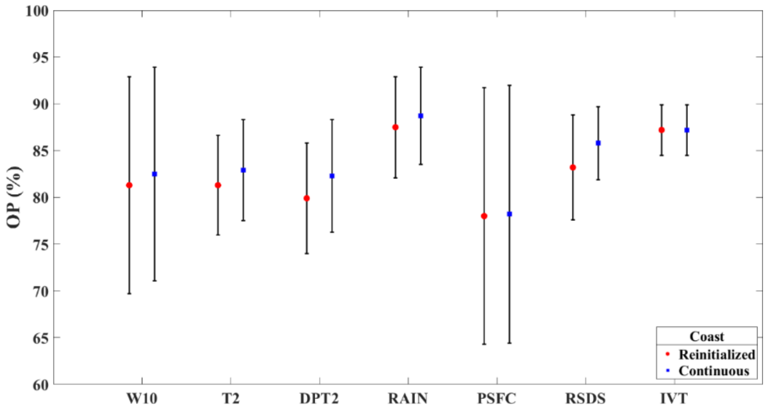

Figure 17. Average OP for the reinitialized (red circles) and continuous (blue squares) simulations, and standard deviations (black lines), over coast areas.

The impact of using CMIP6 instead of ERA5 data is heterogeneous. For both downscaling techniques, OP decreases by 2% for PSFC and 3% for IVT, while RSDS remains unchanged. In the reinitialized and continuous simulations, OP reductions of 2% and 3% were observed for W10, and 2% and 1% for RAIN, respectively. Notably, in the continuous simulation, OP increase by 4% for T2 and 6% for DPT2, whereas in the reinitialized simulation, OP decrease by approximately 6% and 8%. However, it is important to highlight that when using ERA5 data, the continuous simulation initially showed lower OP values than the reinitialized simulation for these two variables (see sections 3.1.2 and 3.1.3). Regarding STDs, the continuous simulation shows reductions of 5% for T2 and 10% for DPT2, while PSFC decreases by about 1% in both techniques. No changes are observed for RSDS in either method or for IVT in the reinitialized simulation. Lastly, all other variables and downscaling techniques, STD increases remain below 2% compared to the ERA5-driven simulations.

Figure 18 presents the average OP over land areas for each of the seven atmospheric variables analysed, along with their respective standard deviations. While both simulation techniques produce similar results, the continuous method generally yields higher OP values, although these differences remain within the range of the STDs for all variables (Table 8). Once again all OPs are above, or close to, the 80%.

https://doi.org/10.5194/egusphere-2025-1339
Preprint. Discussion started: 28 March 2025

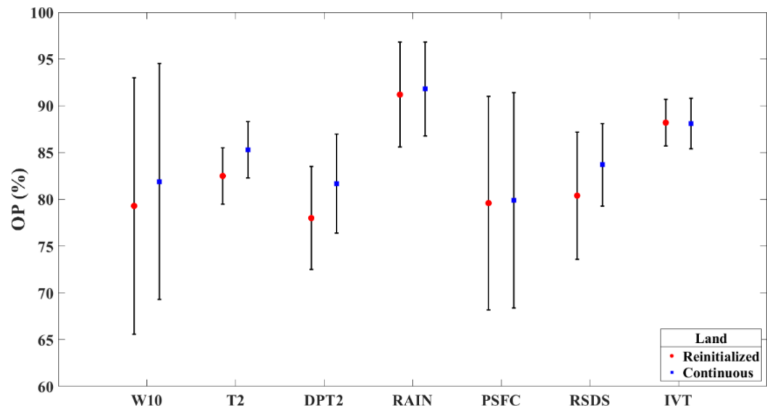

Figure 18. Average OP for the reinitialized (red circles) and continuous (blue squares) simulations, and standard deviations (black lines), over land areas.

Using CMIP6 data instead of ERA5 as input for the WRF model results in a general decrease in OP values. In the reinitialized and continuous simulations, OP decreases by 4% and 2% for W10, 5% and 3% for T2, 10% and 5% for DPT2, 2% and 1% for RAIN, and 3% and 2% for IVT, respectively. For PSFC, both techniques show a 3% decline, while RSDS remains unchanged. The STDs remain largely consistent when using CMIP6 input data. In both simulation techniques, STDs increase by 1% for DPT2 and RAIN and decrease by 1% for PSFC. For W10, the reinitialized simulation shows a 2% increase, while the continuous simulation shows a 1% increase, which also applies to IVT.

Lastly, Figure 19 presents the average OP over mountainous areas for each of the seven atmospheric variables under study, along with their respective standard deviations. W10 and PSFC show relatively low values, around 60%, with corresponding STDs of approximately 20% and 25%, making both simulations unreliable for these variables in mountainous regions. The OPs and the STDs for each downscaling technique are summarized in Table 8. Note that the differences between downscaling techniques fall within the range of the STDs for all variables.

https://doi.org/10.5194/egusphere-2025-1339
Preprint. Discussion started: 28 March 2025

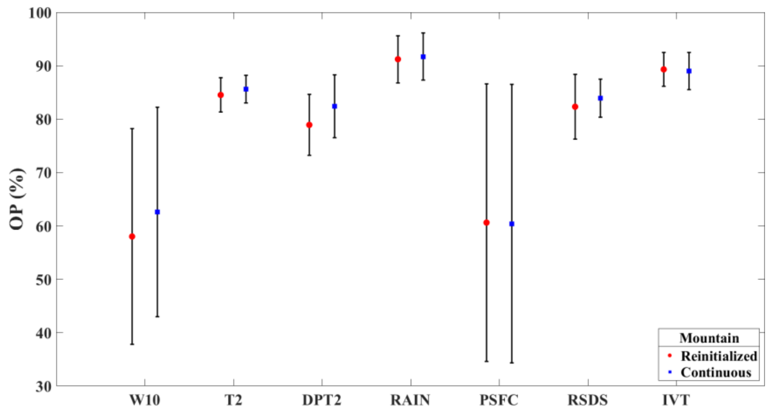

Figure 19. Average OP for the reinitialized (red circles) and continuous (blue squares) simulations, and standard deviations (black lines), over mountain areas.

When using CMIP6 data as input for the WRF model, there is a general decrease or stagnation in OP values, except for RSDS in the reinitialized simulation, where a 1% increase is observed. Specifically, OP decreases by 2% for T2, 9% for DPT2, and 1% for IVT in the reinitialized simulation. For the continuous simulation, decreases are 2% for T2, 5% for DPT2, and 2% for IVT. Regarding STDs, they are generally similar for both techniques, except for DPT2, where they increase by 2% in the reinitialized simulation and 1% in the continuous simulation.

4. Conclusion

Despite the valuable global climate projections provided by GCMs, their coarse spatial resolution limits their applicability for regional studies. RCMs address this limitation through dynamical downscaling, typically performed via continuous simulations or, alternatively, multiple re-initialized simulations over shorter intervals. Each approach has strengths and limitations: the re-initialized method minimizes error accumulation and drastically reduces computational costs, though it may restrict the development of certain atmospheric phenomena. This study applied the WRF model to evaluate continuous and daily re-initialized dynamical downscaling approaches, using ERA5 and CMIP6 data at 1° and 1.25º spatial resolution, respectively, downscaled to 20 km. Spectral nudging was incorporated into the continuous simulation, which included a one-month spin-up period, whereas the reinitialized simulation utilized a 12-hour spin-up period. The results were evaluated against ERA5 data at 0.25° resolution for various atmospheric variables, including wind speed, temperature, humidity, precipitation, surface pressure, and solar radiation, for both climatic and instantaneous comparison. The main findings, based on ERA5 forcing of the dynamical downscaling model, are summarized as follows:

https://doi.org/10.5194/egusphere-2025-1339
Preprint. Discussion started: 28 March 2025

- **W10:** Both methods demonstrate excellent performance in marine areas but are unreliable in mountainous regions. In coastal and land areas, they exhibit good climatic correlation with reference data, though instantaneous correlation is moderate.

- **T2 and DPT2:** Both techniques yield excellent and comparable results overall, except in coastal regions where the continuous method produces only moderate outcomes.

- **RAIN:** Climatologically, both methods perform excellently. However, their instantaneous results are moderate.

- **PSFC:** Both approaches deliver similar and good results, with exceptional performance over the ocean. However, they are unreliable in mountainous areas.

- **RSDS:** Both methods provide good results, with the continuous simulation showing a slight advantage.

- **IVT:** Both techniques achieve excellent and comparable results across all scenarios.

When using CMIP6 data as input, the overall patterns remain similar, although the performance is generally lower compared to ERA5 forcing. Although the datasets used for dynamical downscaling and validation come from different sources - which can introduce some bias - no major differences are observed between the two dynamical downscaling techniques, except that the continuous method avoids the lower performance observed, compared to the reinitialized technique, for T2 and DPT2 in coastal areas for ERA5-driven simulations.

Given the significantly lower computational cost of the re-initialized method - approximately 30 times less in this study - it is the preferred option when its performance is comparable to or exceed that of continuous downscaling. This makes it a highly efficient alternative for high-resolution climate modeling without compromising accuracy in many scenarios.

While this study provides detailed insights into the differences between reinitialized and continuous dynamical downscaling, it remains a case-specific analysis. Various factors could influence these findings. For example, employing a different atmospheric model instead of WRF, or altering its sub-grid scale processes parametrization options, might yield distinct results. Likewise, changes in the domain, spatial resolution, or study area could produce varied findings. Additionally, modifying the reinitialization frequency (other than the daily interval used here) or adjusting the spin-up period for both techniques, could likely influence the results, and alter the computational cost ratio. Finally, although this analysis focuses on key atmospheric variables, expanding the study to include others could reveal further differences between downscaling approaches.

https://doi.org/10.5194/egusphere-2025-1339
Preprint. Discussion started: 28 March 2025

Data availability

The WRF model, used to perform the dynamical downscalings, can be downloaded from the UCAR website (https://www2.mmm.ucar.edu/wrf/users/download/get_source.html). Post-Processing was performed using MATLAB, which can be downloaded from the MathWorks website (https://www.mathworks.com/products/matlab.html). Codes required to conduct the analyses are available at https://doi.org/10.5281/zenodo.15091479 (Thomas, 2025). All data used in this study are publicly available. The multi-model ensemble CMIP6 data (Xu et al., 2021) can be downloaded from the Science Data Bank (https://doi.org/10.11922/sciencedb.00487). ERA5 data (Hersbach et al., 2020) can be downloaded from the Copernicus Climate Data Store (https://doi.org/10.24381/cds.adbb2d47)

Author Contribution

B. Thomas: Conceptualization, Methodology, Software, Validation, Formal analysis, Data curation, Writing – Original Draft, Visualization. **JC. Fernández-Alvarez**: Conceptualization, Methodology, Software, Data curation, Writing – Review & Editing. **X. Costoya**: Conceptualization, Writing – Review & Editing, Supervision. **M. deCastro**: Conceptualization, Resources, Writing – Review & Editing, Supervision. **R. Nieto**: Conceptualization, Supervision. **D.Carvalho**: Methodology, Writing – Review & Editing. **L. Gimeno**: Conceptualization, Supervision. **M. Gómez-Gesteira**: Conceptualization, Resources, Writing – Review & Editing, Supervision.

Declaration of Competing Interest

The authors declare that they have no known competing financial interests or personal relationships that could have appeared to influence the work reported in this paper.

Acknowledgements

This work was partially supported by Xunta de Galicia under project ED431C 2021/44 (Grupos de Referencia Competitiva) and Project CienciasMariñas-MRR C286 (Programa de Ciencias Mariñas BDNS20 654075) funded by the “European Union NextGenerationEU/PRTR C17, i1”. This work has also been supported by the research projects TED2021-129152B-C41 and PID2022-137244OB-I00, financed by the Spanish Ministry of Science and FEDER. In addition, thanks are due to FCT/MCTES for the financial support to CESAM (UIDP/50017/2020 + UIDB/50017/2020 + LA/P/0094/2020). This work was financed by National Funds through the FCT - Fundação para a Ciência e Tecnologia (Portuguese Foundation for Science and Technology) within the project ClimACT (https://doi.org/10.54499/2022.01896.PTDC).

X. Costoya is funded by Grant RYC2023-043509-I (Ramón y Cajal contract) funded by MCIN/AEI/ 10.13039/501100011033 and by the FSE+. JC. Fernández-Alvarez. thanks the support from the Xunta de Galicia (Consellería de Cultura, Educación e Universidade) under the Postdoctoral grant IN606B2024/016. D. Carvalho acknowledges the FCT (Portuguese Foundation for Science and Technology) and the Ministry of Science, Technology and Higher Education (MCTES) for his researcher contract with the reference CEECINST/00013/2021/CP2779/CT0017 (https://doi.org/10.54499).

This research project was made possible through the access granted by the Galician Supercomputing Center (CESGA) to its supercomputing infrastructure. The supercomputer FinisTerrae III and its permanent data storage system have been funded by the Spanish Ministry of Science and Innovation, the Galician Government and the European Regional Development Fund (ERDF). Funding for open access charge: Universidade de Vigo/CISUG.

During the preparation of this work the authors used ChatGPT-3.5 in order to improve language and readability. After using this tool/service, the authors reviewed and edited the content as needed and take full responsibility for the content of the publication.

Appendix

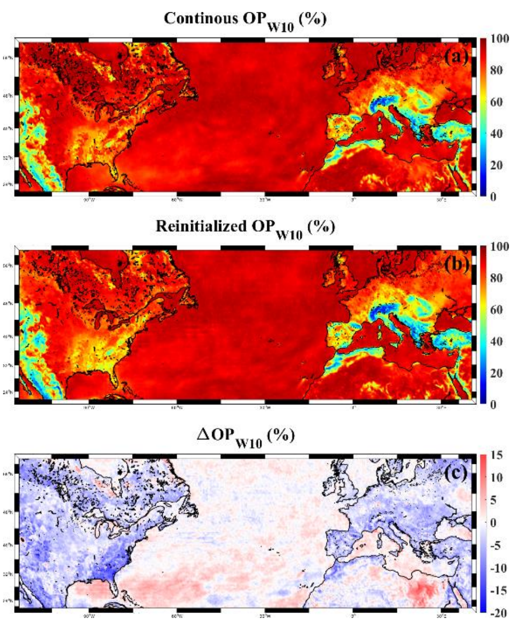

Figure A1. W10 variable: OP between CMIP6-driven WRF simulated data and 0.25º-ERA5 data for the (a) continuous and (b) reinitialized simulations, and (c) difference between the two methods.

https://doi.org/10.5194/egusphere-2025-1339
Preprint. Discussion started: 28 March 2025

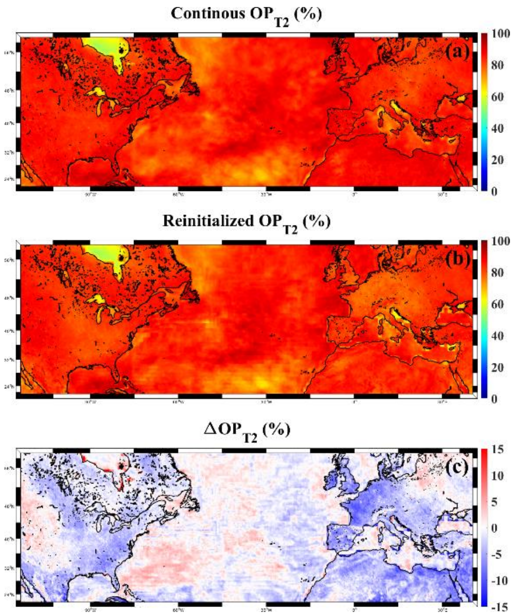

Figure A2. T2 variable: OP between CMIP6-driven WRF simulated data and 0.25°-ERA5 data for the (a) continuous and (b) reinitialized simulations, and (c) difference between the two methods.

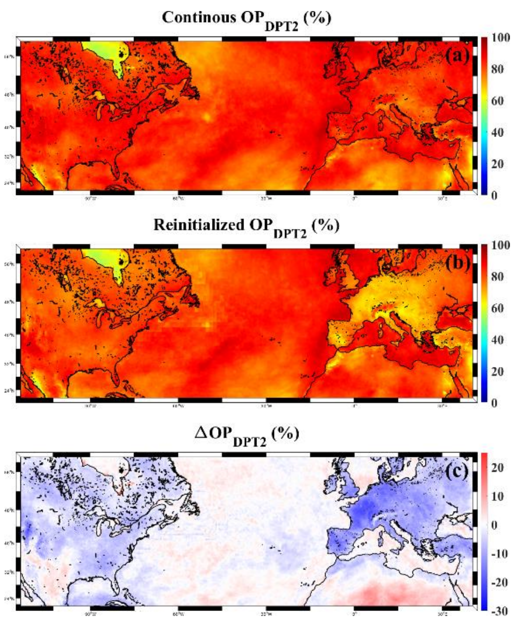

Figure A3. DPT2 variable: OP between CMIP6-driven WRF simulated data and 0.25°-ERA5 data for the (a) continuous and (b) reinitialized simulations, and (c) difference between the two methods.

https://doi.org/10.5194/egusphere-2025-1339
Preprint. Discussion started: 28 March 2025

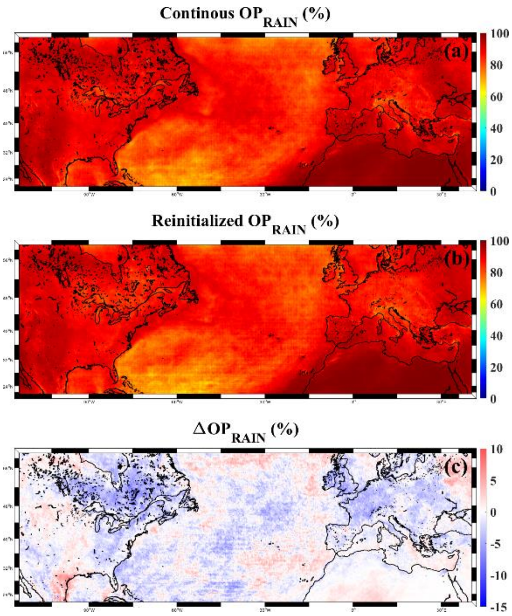

Figure A4. RAIN variable: OP between CMIP6-driven WRF simulated data and 0.25º-ERA5 data for the (a) continuous and (b) reinitialized simulations, and (c) difference between the two methods.

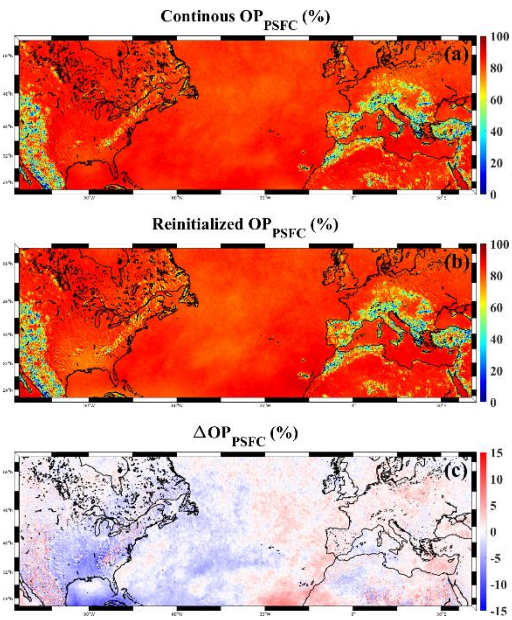

Figure A5. PSFC variable: OP between CMIP6-driven WRF simulated data and 0.25º-ERA5 data for the (a) continuous and (b) reinitialized simulations, and (c) difference between the two methods.

https://doi.org/10.5194/egusphere-2025-1339
Preprint. Discussion started: 28 March 2025

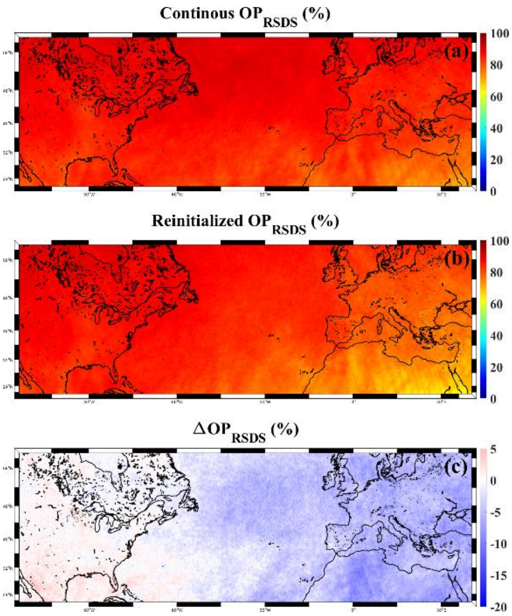

Figure A6. RSDS variable: OP between CMIP6-driven WRF simulated data and 0.25º-ERA5 data for the (a) continuous and (b) reinitialized simulations, and (c) difference between the two methods.

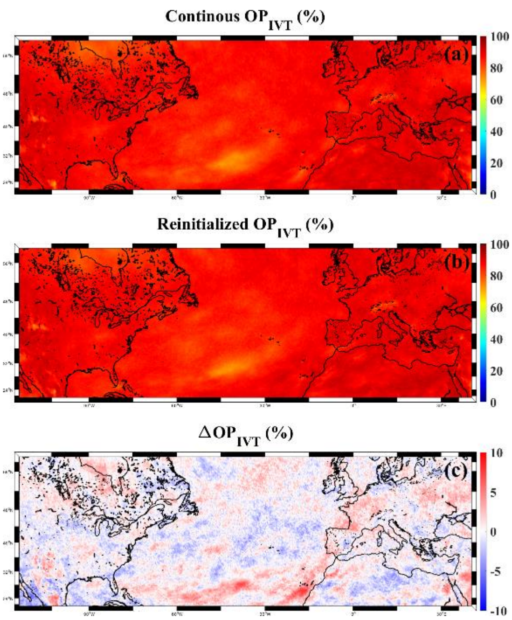

Figure A7. IVT variable: OP between CMIP6-driven WRF simulated data and 0.25º-ERA5 data for the (a) continuous and (b) reinitialized simulations, and (c) difference between the two methods.

https://doi.org/10.5194/egusphere-2025-1339
Preprint. Discussion started: 28 March 2025

References

Bullock, O. R., Alapaty, K., Herwehe, J. A., Mallard, M. S., Otte, T. L., Gilliam, R. C., & Nolte, C. G. (2014). An observation-based investigation of nudging in WRF for downscaling surface climate information to 12-km grid spacing. Journal of Applied Meteorology and Climatology, 53(1), 20-33. https://doi.org/10.1175/JAMC-D-13-030.1

Carvalho, D., Rocha, A., Gómez-Gesteira, M., & Santos, C. (2012). A sensitivity study of the WRF model in wind simulation for an area of high wind energy. Environmental Modelling & Software, 33, 23-34. https://doi.org/10.1016/j.envsoft.2012.01.019

Christensen, O. B. (1999). Relaxation of soil variables in a regional climate model. Tellus A, 51(5), 674-685. https://doi.org/10.1034/j.1600-0870.1999.00010.x

Costoya, X., DeCastro, M., Santos, F., Sousa, M. C., & Gómez-Gesteira, M. (2019). Projections of wind energy resources in the Caribbean for the 21st century. Energy, 178, 356-367. https://doi.org/10.1016/j.energy.2019.04.121

Costoya, X., DeCastro, M., Carvalho, D., & Gómez-Gesteira, M. (2020). On the suitability of offshore wind energy resource in the United States of America for the 21st century. Applied Energy, 262, 114537. https://doi.org/10.1016/j.apenergy.2020.114537

Costoya, X., DeCastro, M., Carvalho, D., Arguilé-Pérez, B., & Gómez-Gesteira, M. (2022). Combining offshore wind and solar photovoltaic energy to stabilize energy supply under climate change scenarios: A case study on the western Iberian Peninsula. Renewable and Sustainable Energy Reviews, 157, 112037. https://doi.org/10.1016/j.rser.2021.112037

Costoya, X., Decastro, M., Carvalho, D., & Gómez-Gesteira, M. (2023). Assessing the complementarity of future hybrid wind and solar photovoltaic energy resources for North America. Renewable and Sustainable Energy Reviews, 173, 113101. https://doi.org/10.1016/j.rser.2022.113101

Deng, A., Stauffer, D. R., Dudhia, J., Otte, T. L., & Hunter, G. K. (2007, June). Update on analysis nudging FDDA in WRF-ARW. In Proceedings of the 8th WRF Users' Workshop (p. 35). https://pdfs.semanticscholar.org/e6a5/6c1e644f6dd6483959d4fc9b287ff6417fd2.pdf [Accessed March 17th 2025]

https://doi.org/10.5194/egusphere-2025-1339
Preprint. Discussion started: 28 March 2025

Eyring, V., Bony, S., Meehl, G. A., Senior, C. A., Stevens, B., Stouffer, R. J., & Taylor, K. E. (2016). Overview of the Coupled Model Intercomparison Project Phase 6 (CMIP6) experimental design and organization. Geoscientific Model Development, 9(5), 1937-1958. https://doi.org/10.5194/gmd-9-1937-2016

Fernández-Alvarez, J. C., Vázquez, M., Pérez-Alarcón, A., Nieto, R., & Gimeno, L. (2023a). Comparison of moisture sources and sinks estimated with different versions of FLEXPART and FLEXPART-WRF models forced with ECMWF reanalysis data. Journal of Hydrometeorology, 24(2), 221-239. https://doi.org/10.1175/JHM-D-22-0018.1

Fernández-Alvarez, J. C., Costoya, X., Pérez-Alarcón, A., Rahimi, S., Nieto, R., & Gimeno, L. (2023b). Dynamical downscaling of wind speed over the North Atlantic Ocean using CMIP6 projections: implications for offshore wind power density. Energy Reports, 9, 873-885. https://doi.org/10.1016/j.egyr.2022.12.036

Gimeno, L., Drumond, A., Nieto, R., Trigo, R. M., & Stohl, A. (2010). On the origin of continental precipitation. Geophysical Research Letters, 37(13). https://doi.org/10.1029/2010GL043712

Glisan, J. M., Gutowski, W. J., Cassano, J. J., & Higgins, M. E. (2013). Effects of spectral nudging in WRF on Arctic temperature and precipitation simulations. Journal of Climate, 26(12), 3985-3999. https://doi.org/10.1175/JCLI-D-12-00318.1

Hersbach, H., Bell, B., Berrisford, P., Hirahara, S., Horányi, A., Muñoz-Sabater, J., ... & Thépaut, J. N. (2020). The ERA5 global reanalysis. Quarterly Journal of the Royal Meteorological Society, 146(730), 1999-2049. https://doi.org/10.1002/qj.3803

Hong, S. Y., & Lim, J. O. J. (2006). The WRF single-moment 6-class microphysics scheme (WSM6). Asia-Pacific Journal of Atmospheric Sciences, 42(2), 129-151. https://www.researchgate.net/profile/Song-You-Hong/publication/331192569_Hongandlim-JKMS-2006/links/5c6b581f92851c1c9dea9d10/Hongandlim-JKMS-2006.pdf?_sg%5B0%5D=started_experiment_milestone&origin=journalDetail&_rtd=e30%3D [Accessed March 17th 2025]

Hong, S. Y., Noh, Y., & Dudhia, J. (2006). A new vertical diffusion package with an explicit treatment of entrainment processes. Monthly Weather Review, 134(9), 2318-2341. https://doi.org/10.1175/MWR3199.1

Horvath, K., Koracin, D., Vellore, R., Jiang, J., & Belu, R. (2012). Sub-kilometer dynamical downscaling of near-surface winds in complex terrain using WRF and MM5 mesoscale models. Journal of Geophysical Research: Atmospheres, 117(D11). https://doi.org/10.1029/2012JD017432

Iacono, M. J., Delamere, J. S., Mlawer, E. J., Shephard, M. W., Clough, S. A., & Collins, W. D. (2008). Radiative forcing by long-lived greenhouse gases: Calculations with the AER radiative transfer models. Journal of Geophysical Research: Atmospheres, 113(D13). https://doi.org/10.1029/2008JD009944

Insua-Costa, D., & Miguez-Macho, G. (2018). A new moisture tagging capability in the Weather Research and Forecasting model: formulation, validation and application to the 2014 Great Lake-effect snowstorm. Earth System Dynamics, 9(1), 167-185. https://doi.org/10.5194/esd-9-167-2018

Insua-Costa, D., Miguez-Macho, G., & Llasat, M. C. (2019). Local and remote moisture sources for extreme precipitation: a study of the two catastrophic 1982 western Mediterranean episodes. Hydrology and Earth System Sciences, 23(9), 3885-3900. https://doi.org/10.5194/hess-23-3885-2019

IPCC (2021). Climate Change 2021 - The Physical Science Basis - Summary for Policymakers. https://www.ipcc.ch/report/ar6/wg1/downloads/report/IPCC_AR6_WGI_SPM_final.pdf [Accessed March 17th 2025]

Jacob, D., Petersen, J., Eggert, B., Alias, A., Christensen, O. B., Bouwer, L. M., ... & Yiou, P. (2014). EURO-CORDEX: new high-resolution climate change projections for European impact research. Regional Environmental Change, 14, 563-578. https://doi.org/10.1007/s10113-013-0499-2

Jerez, S., López-Romero, J. M., Turco, M., Lorente-Plazas, R., Gómez-Navarro, J. J., Jiménez-Guerrero, P., & Montávez, J. P. (2020). On the spin-up period in WRF simulations over Europe: Trade-offs between length and seasonality. Journal of Advances in Modeling Earth Systems, 12(4), e2019MS001945. https://doi.org/10.1029/2019MS001945

Jiménez, P. A., Dudhia, J., González-Rouco, J. F., Navarro, J., Montávez, J. P., & García-Bustamante, E. (2012). A revised scheme for the WRF surface layer formulation. Monthly Weather Review, 140(3), 898-918. https://doi.org/10.1175/MWR-D-11-00056.1

Kain, J. S. (2004). The Kain–Fritsch convective parameterization: an update. Journal of Applied Meteorology and Climatology, 43(1), 170-181. https://doi.org/10.1175/1520-0450(2004)043%3C0170:TKCPAU%3E2.0.CO;2

Liu, P., Qiu, X., Yang, Y., Ma, Y., & Jin, S. (2018). Assessment of the performance of three dynamical climate downscaling methods using different land surface information over China. Atmosphere, 9(3), 101. https://doi.org/10.3390/atmos9030101

Lo, J. C. F., Yang, Z. L., & Pielke Sr, R. A. (2008). Assessment of three dynamical climate downscaling methods using the Weather Research and Forecasting (WRF) model. Journal of Geophysical Research: Atmospheres, 113(D9). https://doi.org/10.1029/2007JD009216

Lucas-Picher, P., Boberg, F., Christensen, J. H., & Berg, P. (2013). Dynamical downscaling with reinitializations: A method to generate finescale climate datasets suitable for impact studies. Journal of Hydrometeorology, 14(4), 1159-1174. https://doi.org/10.1175/JHM-D-12-063.1

Miguez-Macho, G., Stenchikov, G. L., & Robock, A. (2004). Spectral nudging to eliminate the effects of domain position and geometry in regional climate model simulations. Journal of Geophysical Research: Atmospheres, 109(D13). https://doi.org/10.1029/2003JD004495

Pan, Z., Takle, E., Gutowski, W., & Turner, R. (1999). Long simulation of regional climate as a sequence of short segments. Monthly Weather Review, 127(3), 308-321. https://doi.org/10.1175/1520-0493(1999)127%3C0308:LSORCA%3E2.0.CO;2

Perkins, S. E., Pitman, A. J., Holbrook, N. J., & McAneney, J. (2007). Evaluation of the AR4 climate models' simulated daily maximum temperature, minimum temperature, and precipitation over Australia using probability density functions. Journal of Climate, 20(17), 4356-4376. https://doi.org/10.1175/JCLI4253.1

Qian, J. H., Seth, A., & Zebiak, S. (2003). Reinitialized versus continuous simulations for regional climate downscaling. Monthly Weather Review, 131(11), 2857-2874. https://doi.org/10.1175/1520-0493(2003)131%3C2857:RVCSFR%3E2.0.CO;2

Ratna, S. B., Cherchi, A., Joseph, P. V., Behera, S. K., Abish, B., & Masina, S. (2016). Moisture variability over the Indo-Pacific region and its influence on the Indian summer monsoon rainfall. Climate Dynamics, 46, 949-965. https://doi.org/10.1007/s00382-015-2624-z

Riahi, K., Van Vuuren, D. P., Kriegler, E., Edmonds, J., O'neill, B. C., Fujimori, S., ... & Tavoni, M. (2017). The Shared Socioeconomic Pathways and their energy, land use, and greenhouse gas emissions implications: An overview. Global Environmental Change, 42, 153-168. https://doi.org/10.1016/j.gloenvcha.2016.05.009

Schewe, J., Gosling, S. N., Reyer, C., Zhao, F., Ciais, P., Elliott, J., ... & Warszawski, L. (2019). State-of-the-art global models underestimate impacts from climate extremes. Nature Communications, 10(1), 1005. https://doi.org/10.1038/s41467-019-08745-6

Seck, A., Welty, C., & Maxwell, R. M. (2015). Spin-up behavior and effects of initial conditions for an integrated hydrologic model. Water Resources Research, 51(4), 2188-2210. https://doi.org/10.1002/2014WR016371

Skamarock, W. C., Klemp, J. B., Dudhia, J., Gill, D. O., Liu, Z., Berner, J., ... & Huang, X. Y. (2021). A Description of the Advanced Research WRF Model Version 4.3; No. NCAR/TN556+ STR. https://doi.org/10.5065/1dfh-6p97

Spero, T. L., Nolte, C. G., Mallard, M. S., & Bowden, J. H. (2018). A maieutic exploration of nudging strategies for regional climate applications using the WRF model. Journal of Applied Meteorology and Climatology, 57(8), 1883-1906. https://doi.org/10.1175/JAMC-D-17-0360.1

Spero, T. L., Otte, M. J., Bowden, J. H., & Nolte, C. G. (2014). Improving the representation of clouds, radiation, and precipitation using spectral nudging in the Weather Research and Forecasting model. Journal of Geophysical Research: Atmospheres, 119(20), 11-682. https://doi.org/10.1002/2014JD022173

Taylor, K. E. (2001). Summarizing multiple aspects of model performance in a single diagram. Journal of Geophysical Research: Atmospheres, 106(D7), 7183-7192. https://doi.org/10.1029/2000JD900719

Tewari, M., Chen, F., Wang, W., Dudhia, J., LeMone, M. A., Mitchell, K., … & Cuenca, R. H. (2004). Implementation and verification of the unified noah land surface model in the WRF model. Bulletin of the American Meteorololgical Society, 2165-2170. https://www.scopus.com/record/display.uri?eid=2-s2.0-2442555920&origin=inward [Accessed March 17th 2025]

Thomas, B., Costoya, X., Decastro, M., Insua-Costa, D., Senande-Rivera, M., & Gómez-Gesteira, M. (2023). Downscaling CMIP6 climate projections to classify the future offshore wind energy resource in the Spanish territorial waters. Journal of Cleaner Production, 433, 139860. https://doi.org/10.1016/j.jclepro.2023.139860

Thomas, B., Costoya, X., Decastro, M., Iglesias, G., & Gómez-Gesteira, M. (2025). Forecasting offshore wind energy in Atlantic Europe using CMIP6 dynamically downscaled data. Energy [Under Review].

https://doi.org/10.5194/egusphere-2025-1339
Preprint. Discussion started: 28 March 2025

Thomas, B. (2025). Comparative Analysis of Continuous and Reinitialized Dynamical Downscaling in the North Atlantic and Surrounding Continents [Code]. https://doi.org/10.5281/zenodo.15091479

Wootten, A., Bowden, J. H., Boyles, R., & Terando, A. (2016). The sensitivity of WRF downscaled precipitation in Puerto Rico to cumulus parameterization and interior grid nudging. Journal of Applied Meteorology and Climatology, 55(10), 2263-2281. https://doi.org/10.1175/JAMC-D-16-0121.1

WRF Users Page (2024). WPS V4 Geographical Static Data. https://www2.mmm.ucar.edu/wrf/users/download/get_sources_wps_geog.html [Accessed March 17th 2025]

Xu, Z., Han, Y., Tam, C. Y., Yang, Z. L., & Fu, C. (2021). Bias-corrected CMIP6 global dataset for dynamical downscaling of the historical and future climate (1979–2100). Scientific Data, 8(1), 293. https://doi.org/10.1038/s41597-021-01079-3

Zhang, S., & Li, X. (2021). Future projections of offshore wind energy resources in China using CMIP6 simulations and a deep learning-based downscaling method. Energy, 217, 119321. https://doi.org/10.1016/j.energy.2020.119321